PHILOSOPHICAL TRANSACTIONS OF THE ROYAL SOCIETY A MATHEMATICAL, PHYSICAL & ENGINEERING SCIENCES

The Interaction of Large Amplitude Barotropic Waves with an Ambient Shear Flow: Critical Flows

E. Varley, J. Y. Kazakia and P. A. Blythe

Phil. Trans. R. Soc. Lond. A 1977 **287**, 189-236
doi: 10.1098/rsta.1977.0144

THE INTERACTION OF LARGE AMPLITUDE BAROTROPIC WAVES WITH AN AMBIENT SHEAR FLOW: CRITICAL FLOWS

By E. VARLEY, J. Y. KAZAKIA and P. A. BLYTHE
Centre for the Application of Mathematics, Lehigh University
Bethlehem, Pennsylvania 18015

(*Communicated by Sir James Lighthill F.R.S.* – *Received* 14 *June* 1976 –
Revised 6 *December* 1976)

CONTENTS

Vol. 287. A 1342. 24 [Published 4 October 1977

This study discusses the evolution of long gravity waves on shear flows. Although the paper is concerned mainly with finite amplitude neutrally stable flows which contain a critical level, a new representation is given for the unstable mode solutions of the linearized equations. From these solutions it appears that focusing instabilities, usually associated with nonlinear viscous effects, can occur even in linear inviscid theory.

For finite amplitude disturbances the analysis is restricted to polygonal shear profiles and only the neutrally stable solutions are considered. The theory is presented in detail for a simple two-layer profile which can support a critical mode. At small Froude numbers the critical mode is essentially an internal wave. This limiting solution also describes critical flows between parallel rigid boundaries when there is no body force.

The finite amplitude solutions are generalizations of the classical simple wave solutions for unsheared flows. As in the classical case, those waves can break but it is found that the conditions under which they break can be markedly different for shear flows. Calculations for the particle trajectories are also presented. These trajectories differ from the usual Kelvin's cat's eye pattern in that they are, in general, no longer closed.

Finally, it is observed that there are many other barotropic flows for which the governing equations can be reduced to a form equivalent to the shallow water equations discussed here. A list of such flows is given.

1. INTRODUCTION

This paper describes the propagation of large amplitude shallow-water gravity waves over a horizontal bed into a region where the flow is sheared in a vertical direction. It is mainly concerned with neutrally stable waves for which the flow contains a critical level where the horizontal component of fluid velocity u and the wave speed c coincide. These waves contain trapped particles whose trajectories are generalizations of the famous Kelvin's cat's eyes. Now though, because of the effect of non-linearity, these trajectories do not usually form closed orbits but distort as the particles are convected with the wave. The waves may be of infinite horizontal extent or they may be separated by sharp fronts from regions of steady parallel flow where the fluid is sheared in a vertical, but not in a horizontal, direction.

Although the terminology used in this paper is that associated with shallow-water waves, the results obtained are directly applicable to many other barotropic flows that involve the interaction of long waves with ambient flows that are sheared in a direction transverse to the direction of wave propagation: the equations governing many of these flows can be transformed into a form that is almost identical to those governing shallow-water waves. A list of such flows, together with the appropriate transformations, is given in §10. Included are flows produced by atmospheric gravity waves in a barotropic (well mixed) atmosphere as well as flows of compressible and incompressible fluids down ducts or down tubes with flexible walls.

The equations governing the propagation of shallow-water gravity waves on a sheared flow are stated in §2. These equations have solutions describing steady parallel shear flows for which the

horizontal component of the fluid velocity u, $= U_0(y)$, is an arbitrary function of the vertical distance measure y but is independent of x, the distance measure in the horizontal direction. For these flows the vertical component of fluid velocity $v \equiv 0$ while the fluid depth H is constant. When the governing equations are formally linearized about these steady flow solutions the resulting equations have two types of solution for which the dependence of the flow variables on y separates from their dependence on (x, t). For the first kind, which describe neutrally stable disturbances, $H(x, t)$ satisfies the one-dimensional progressing wave equation

$$\frac{\partial H}{\partial t} + c_0 \frac{\partial H}{\partial x} = 0 \tag{1.1}$$

for some constant c_0. For the second kind of solution, which describes unstable waves, H satisfies the equation

$$\frac{\partial^2 H}{\partial t^2} + c_{02}^2 \frac{\partial^2 H}{\partial \alpha^2} = 0 \quad \text{where} \quad \alpha = x - c_{01} t \tag{1.2}$$

and (c_{01}, c_{02}) are constants. In general, there are two different kinds of unstable disturbances governed by (1.2): those that become unbounded at all x as $t \to \infty$ or those that focus and become unbounded at a definite horizontal position at a definite time. Examples of both kinds of instability are given in §2.3 when the initial disturbance contains infinite energy, as it does when H is periodic in x at $t = 0$, and when the initial disturbance contains finite energy. (These instabilities are illustrated in figures 1*a*, *b*, §2.) Focusing instabilities caused by nonlinear and viscous effects have been discussed previously by Hocking, Stewartson & Stuart (1972) and by Davey, Hocking & Stewartson (1974). However, the instabilities discussed by these authors have a different structure from those discussed here: in their analysis the wave envelope is singular, in ours it is the wave profile that is singular.

For finite amplitude waves the dependence of the flow variables on y cannot usually be computed independently of their dependence on (x, t), as it can for the small amplitude waves discussed in §2. However, there is a class of flows for which the dependence of the flow variables on y is immediately apparent and only their dependence on (x, t) must be calculated. These flows are characterized by the fact that the shear profile at some vertical cross-section, which is traversed by all particles in the flow, is always of the polygonal form shown in figure 2. It then follows that the flow consists of layers, separated by fluid interfaces, in each of which u is of the form

$$u = \omega y + \bar{u}(x, t), \tag{1.3}$$

where $\bar{u}(x, t)$ and the constant ω, which is the hydraulic flow approximation to the horizontal component of vorticity, differ from layer to layer. In this paper, in order to analyse the *broad* features of shear flows containing a critical level, we consider such layered flows. Although it might be thought that this investigation would yield anomalous results, as it automatically assumes that

$$\partial^2 u / \partial y^2 = 0 \quad \text{at the critical level,} \tag{1.4}$$

in a subsequent paper we show that during the passage of a wave the shear profile *always* adjusts so that (1.4) holds. Most of the major flow features associated with the presence of a critical level are correctly predicted by the polygonal model. There is, however, one important exception. In the small amplitude limit when (1.4) does not hold ahead of the wave there is an amplification to the perturbation of u at the critical level which is proportional to

$$\kappa = g \frac{\partial^2 u}{\partial y^2} \Big/ \left(\frac{\partial u}{\partial y}\right)^3, \tag{1.5}$$

PHILOSOPHICAL TRANSACTIONS OF THE ROYAL SOCIETY A MATHEMATICAL, PHYSICAL & ENGINEERING SCIENCES

where the derivatives are computed at the critical level just ahead of the wave. This phenomenon is not predicted when the shear profile is assumed to be polygonal for then $\kappa = 0$.

The full nonlinear equations governing $H(x,t)$ and $\bar{u}(x,t)$ are derived in §3.1. In §3.2 we show how the general solution to the linearized equations can be represented as a sum of all the possible neutrally stable and unstable mode solutions. These solutions can satisfy prescribed initial conditions on the $\bar{u}$.

The large amplitude generalizations of the neutrally stable waves are presented in §4. These are described by simple wave solutions to the equations governing $H(x,t)$ and the $\bar{u}(x,t)$. For these solutions $\bar{u} = \bar{u}(H)$, so that (1.3) reads

$$u = \omega y + \bar{u}(H), \tag{1.6}$$

where $H(x,t)$ satisfies the nonlinear progressing wave equation

$$\frac{\partial H}{\partial t} + c(H)\frac{\partial H}{\partial x} = 0. \tag{1.7}$$

It is pointed out in §4.2 that solutions of the form (1.6) and (1.7) are special examples of a more general class of exact solutions to the nonlinear shallow-water equations for which H satisfies (1.7) while u and v can be written in the similarity form

$$u = U(H,y) \quad \text{and} \quad v = (\partial H/\partial x)\, V(H,y). \tag{1.8}$$

These solutions, which describe the interaction of neutrally stable waves with any ambient shear profile, were first obtained by Blythe, Kazakia & Varley (1971, 1972) in their study of flows that do not contain a critical level. In a subsequent paper the representation (1.8) will be used to describe the effect of non-zero κ on the flow near a critical level.

In this paper we discuss large amplitude neutrally stable modes only when the shear profile is polygonal. Generally, there is more than one such mode for which this profile takes a specified form at some vertical cross-section where $H = H_0$. Each such mode can be characterized by the value of $c_0 = c(H_0)$ which is the velocity with which the depth $H = H_0$ would propagate in a disturbance caused by exciting just that mode. When the polygonal profile consists of n layers, with different values of ω in adjacent layers, all possible values of c_0 are roots of an $(n+1)^{\text{th}}$ degree polynomial whose coefficients are determined by the geometry of the shear profile at $H = H_0$. There are as many neutrally stable modes as there are real roots of this polynomial. The complex roots correspond to unstable modes. Unfortunately, any finite amplitude disturbance cannot be regarded as a composite of these modes, as can a small amplitude disturbance, since these modes usually interact. Consequently, an analysis of the flow produced by a single finite amplitude mode is only of immediate physical relevance when it can be argued that this mode contains most of the energy of the disturbance. This occurs, for example, when the flow is stable and the disturbance is initially limited to a finite interval of the x-axis. Althogh the different neutrally stable modes initially interact, they will ultimately separate since they are moving at different speeds. At some later time the flow consists of isolated modes separated by regions of uniform parallel shear flow.

As an illustration of the general analysis, the case of a simple two layered shear profile that can support a critical mode (see figure 3*a*) is discussed at length in §§5–9. This flow is always stable (there is no unstable mode) and can support three neutrally stable modes: one for which the flow is wholly subcritical, one for which the flow is wholly supercritical, and one for which the flow contains both subcritical and supercritical flow regions. For the critical mode the level $y = y_c(H)$, at which $u = c(H)$, always lies in the lower (sheared) layer. The flow is subcritical below, and

PHILOSOPHICAL TRANSACTIONS OF THE ROYAL SOCIETY A MATHEMATICAL, PHYSICAL & ENGINEERING SCIENCES

supercritical above, this level. An analysis of all three families of waves is given in appendix A. In the main body of the paper we discuss in detail the limiting case of internal waves which occur when

$$\omega^2 H/g \to 0. \tag{1.9}$$

In this limit the speeds of the subcritical and supercritical modes relative to the flow are infinitely large compared with the speed of the critical mode, and it is shown in § 6.3 that the most general flow possible can be regarded as that due to a critical mode on which there is superimposed a time varying, but spatially uniform, parallel flow.

Subject to (1.9), simple limiting expressions for $U(H,y)$, $V(H,y)$, $c(H)$ and $y_c(H)$ are derived in § 5.2. It is shown that during the passage of any critical mode the variation in the height of the free surface is negligible compared with the variations in $y_i(H)$, the height of the fluid interface separating the sheared and unsheared layers. In fact, during the passage of a wave, this interface, and the critical level, can travel from the lower to the upper boundary of the flow region with only a second-order change in the level of the free surface. In this sense the critical modes represent internal waves. This is emphasized in § 6, where it is shown that the limiting forms of $u(x,y,t)$ and $v(x,y,t)$ are exact solutions of the equations governing hydraulic flows between two rigid parallel boundaries. These latter flows are discussed briefly in § 6 where it is shown that any neutrally stable mode must contain a critical level.

It is convenient to discuss the flow in terms of the variation in ground pressure p_0. In § 5 it is shown that any decrease in p_0 always causes y_c and y_i to increase. If H_M denotes the maximum depth, a fall of $\frac{1}{12}\rho\omega^2 H_M^2$ in p_0 can drive both these levels from $y = 0$ to $y = H_M$. Thus, since a wave always breaks when the critical level reaches either the upper or the lower boundary of the flow region, the maximum range of variation of p_0 for which the present theory is valid is $\frac{1}{12}\rho\omega^2 H_M^2$.

For gravity waves on an unsheared flow c always increases as p_0 increases. A novel feature of the waves described in §§ 5–9 is that c is not always an increasing function of p_0 (see figure 6). If p_M denotes the pressure at which $y_c = 0$, when

$$0 \leqslant (p_M - p_0) < \tfrac{1}{108}\rho\omega^2 H_M^2, \quad 0 \leqslant y_c \leqslant \tfrac{1}{9}H_M \quad \text{and} \quad \frac{dc}{dp_0} > 0; \tag{1.10}$$

while when

$$\tfrac{1}{108}\rho\omega^2 H_M^2 < (p_M - p_0) \leqslant \tfrac{1}{12}\rho\omega^2 H_M^2, \quad \tfrac{1}{9}H_M < y_c \leqslant H_M \quad \text{and} \quad \frac{dc}{dp_0} < 0. \tag{1.11}$$

Since p_0 satisfies equation (1.7), conditions (1.10) and (1.11) imply that large pressure gradients (which produce large vertical currents) either form in that part of the wave where p_0 lies in the range (1.10) and is increasing at any fixed x during the passage of the wave or where p_0 lies in the range (1.11) and is decreasing. The distortion of a typical wave which contains regions where both conditions (1.10) and (1.11) hold is discussed in § 8 and illustrated in figure 15.

For neutrally stable waves it is possible to calculate the variation in the vertical height of any particle as a function of the ground pressure immediately below it independently of how p_0 varies with (x, t): the images of particle trajectories in the (y, p_0) plane are determined by the shear profile and are independent of the wave profile. The flow pattern for waves containing a critical level is considerably more complex than that for waves where the flow is wholly subcritical or wholly supercritical. For these latter flows particles either enter the wave at its front and, after completely traversing the wave, exit at its back, or enter the wave at the back and exit at its front. By contrast, in a wave containing a critical level there are usually three kinds of particles: those that enter the wave at its front or back and completely traverse it; those that enter the wave

at its front or back but are turned before they can fully traverse the wave to exit at the same side they entered but at a different height; and, finally, there are trapped particles that move up and down, and backward and forwards, but never leave the wave. The trajectories of these trapped particles are generalizations of Kelvin's cat's eyes. In § 7, we obtain simple expressions, which are valid in the limit (1.9), relating the variations in y and p_0 at all three types of particles.

The actual trajectories of particles in the (x, y) plane do, of course, depend on $p_0(x, t)$. Since this function satisfies an equation of the form (1.7), it is determined once $p_0(x, 0)$ is specified. In § 8, subject to (1.9), we obtain expressions for all particle trajectories, together with expressions for the travel times of all particles along them, in terms of $p_0(x, 0)$. In particular, we show that when p_0 is less inside the wave than outside, the wave contains trapped particles. Relative to the wave-front, any such particle oscillates backward and forward between equal pressure levels. Since these pressure levels propagate with the same constant velocity they remain a fixed distance apart. Also, the extreme vertical levels reached by any trapped particle and the time it takes the particle to traverse the distance between its extreme horizontal positions remains unchanged as the particle oscillates. However, although the overall dimensions of a particle's orbit remain unchanged, the orbits do not usually form closed curves as seen by an observer moving with the front since the horizontal positions at which a particle reaches its extreme positions move relative to the front. In fact, as the wave steepens the orbits also steepen until their slopes become unbounded as the wave breaks.

2. Formulation

2.1. *Linear theory*

As an introduction to this study we consider a plane shallow-water gravity wave propagating over a horitonzal bed in a direction of increasing distance measure x. In the wave the horizontal component of fluid velocity $u(x, y, t)$ is related to the vertical component $v(x, y, t)$ and fluid depth $H(x, t)$ by the hydraulic flow, or long wave, equations

$$\frac{\partial u}{\partial t}+u\frac{\partial u}{\partial x}+v\frac{\partial u}{\partial y}+g\frac{\partial H}{\partial x}=0 \tag{2.1}$$

and

$$\frac{\partial u}{\partial x}+\frac{\partial v}{\partial y}=0. \tag{2.2}$$

These are to be solved subject to the conditions that

$$v=0 \quad \text{on} \quad y=0 \tag{2.3}$$

and

$$v=\partial H/\partial t+u\,\partial H/\partial x \quad \text{on the free surface} \quad y=H(x,t). \tag{2.4}$$

The pressure in the fluid

$$p=p_{\mathrm{A}}+\rho g(H-y), \tag{2.5}$$

where p_{A} is the constant pressure on the free surface and ρ is the constant density of the fluid.

Equations (2.1)–(2.4) have trivial solutions describing steady parallel shear flows for which

$$H\equiv\text{constant}, \quad =H_0 \text{ say}, \quad \text{while} \quad [u, v]=[U_0(y), 0], \tag{2.6}$$

where $U_0(y)$ is arbitrary. When equations (2.1)–(2.4) are formally linearized about the solutions (2.6) the resulting equations can be written

$$\frac{\partial u}{\partial t}+U_0\frac{\partial u}{\partial x}+\frac{\mathrm{d}U_0}{\mathrm{d}y}v+g\frac{\partial H}{\partial x}=0 \tag{2.7}$$

and

$$\frac{\partial u}{\partial x}+\frac{\partial v}{\partial y}=0. \tag{2.8}$$

These are to be solved subject to the conditions that

$$v = 0 \quad \text{on} \quad y = 0 \tag{2.9}$$

and

$$v = \frac{\partial H}{\partial t} + U_0 \frac{\partial H}{\partial x} \quad \text{on} \quad y = H_0. \tag{2.10}$$

2.2 *Neutrally stable small amplitude waves*

There are two kinds of solutions to equations (2.7)–(2.10) that describe progressing waves. For the first kind we can write

$$u = U_0(y) + U_1(y)\,(H - H_0) \quad \text{and} \quad v = V_0(y)\frac{\partial H}{\partial x}, \tag{2.11}$$

where $H(x, t)$ satisfies the progressing wave equation

$$\frac{\partial H}{\partial t} + c_0 \frac{\partial H}{\partial x} = 0 \tag{2.12}$$

for some real constant c_0. $V_0(y)$ is determined from the equation

$$(U_0 - c_0)\frac{\mathrm{d}V_0}{\mathrm{d}y} - \frac{\mathrm{d}U_0}{\mathrm{d}y}V_0 = g, \tag{2.13}$$

which must be solved subject to the conditions that

$$V_0 = 0 \quad \text{on} \quad y = 0 \quad \text{and} \quad V_0 = U_0 - c_0 \quad \text{on} \quad y = H_0. \tag{2.14}$$

When (2.13) is differentiated with respect to y it follows that V_0 satisfies the low-frequency Rayleigh equation

$$(U_0 - c_0)\frac{\mathrm{d}^2V_0}{\mathrm{d}y^2} - \frac{\mathrm{d}^2U_0}{\mathrm{d}y^2}V_0 = 0, \tag{2.15}$$

which occurs in studies of hydrodynamic stability (see, for example, Stuart 1963).

When there is no critical level at which $U_0(y) = c_0$ (2.13) and the first of conditions (2.14) imply that

$$V_0 = g(U_0 - c_0)\int_0^y \frac{\mathrm{d}y}{(U_0 - c_0)^2}. \tag{2.16}$$

The second of conditions (2.14) then implies that c_0 must be determined from the relation (Burns 1953)

$$g\int_0^{H_0} \frac{\mathrm{d}y}{(U_0 - c_0)^2} = 1. \tag{2.17}$$

Also,

$$U_1 = -\frac{\mathrm{d}V_0}{\mathrm{d}y} = -g\left[(U_0 - c_0)^{-1} + \frac{\mathrm{d}U_0}{\mathrm{d}y}\int_0^y \frac{\mathrm{d}y}{(U_0 - c_0)^2}\right]. \tag{2.18}$$

The waves described by (2.11), (2.12), (2.16) and (2.18) are all neutrally stable disturbances in the sense that during their passage the total variations in H and $\partial H/\partial x$, and hence in u and v at any fixed y, are identical at all horizontal stations. This property for H and $\partial H/\partial x$ follows directly from (2.12); for u and v it follows from conditions (2.11) which state that u only depends on (x, t) through its dependence on H while v only depends on (x, t) through its dependence on $\partial H/\partial x$.

2.3. *Unstable small amplitude waves*

For certain forms of the shear profile, $U_0(y)$, there is a second class of solutions to equations (2.7)–(2.10) that describe unstable progressing waves. For these solutions we can write

$$u = U_0(y) + U_{11}(y)\,[H(x, t) - H_0] + U_{12}(y)\,L(x, t). \tag{2.19}$$

It then follows from (2.8) and (2.9) that v is of the form

$$v = V_{01}(y)\frac{\partial H}{\partial x} + V_{02}(y)\frac{\partial L}{\partial x}. \tag{2.20}$$

When the expressions (2.19) and (2.20) are inserted in (2.7) it follows that $H(x,t)$ and $L(x,t)$ satisfy the equations

$$\left.\begin{aligned} \frac{\partial H}{\partial t} + c_{01}\frac{\partial H}{\partial x} &= -c_{02}\frac{\partial L}{\partial x}, \\ \frac{\partial L}{\partial t} + c_{01}\frac{\partial L}{\partial x} &= c_{02}\frac{\partial H}{\partial x} \end{aligned}\right\} \tag{2.21}$$

for some real constants c_{01} and c_{02}. Also,

$$U_1(y) = U_{11} + \mathrm{i}U_{12} \quad \text{and} \quad V_0(y) = V_{01} + \mathrm{i}V_{02} \tag{2.22}$$

are still given by (2.16) and (2.18) with the complex constant

$$c_0 = c_{01} + ic_{02} \tag{2.23}$$

determined from condition (2.17). The term involving $L(x, t)$ occurs in (2.19) but not in (2.11) because an unstable mode is usually a composite of two components that are out of phase.

The determination of the conditions that $U_0(y)$ must satisfy for (2.17) to have solutions with $c_{02} \neq 0$ is unresolved. Note, however, that the argument first put forward by Rayleigh 1880 to show that certain shear flows are always stable when $U_0''(y)$ is of one sign for all y is not applicable when the upper boundary of the sheared flow is a free surface. It does follow from (2.17) though that if c_0 satisfies (2.17) so does its complex conjugate $\bar{c}_0$. It is also easy to show that if $c_{02} \neq 0$ there is some level $y = y_c$ at which $c_{01} = U_0(y_c)$.

To analyse the unstable waves it is convenient to use t and the phase variable

$$\alpha = x - c_{01}t \tag{2.24}$$

as independent variables rather than t and x. In terms of these variables equations (2.21) can be written

$$\frac{\partial H}{\partial t} = -c_{02}\frac{\partial L}{\partial \alpha} \quad \text{and} \quad \frac{\partial L}{\partial t} = c_{02}\frac{\partial H}{\partial \alpha}, \tag{2.25}$$

which are in the form of Cauchy–Riemann equations. It then follows that

$$(H - H_0) + \mathrm{i}L = F(z), \tag{2.26}$$

where F is an analytic function of the complex variable

$$z = \alpha + \mathrm{i}c_{02}t. \tag{2.27}$$

Also, for future reference, $H(\alpha, t)$ satisfies the equation

$$\frac{\partial^2 H}{\partial t^2} + c_{02}^2\frac{\partial^2 H}{\partial \alpha^2} = 0, \tag{2.28}$$

which can readily be transformed into Laplace's equation.

Although (2.11) and (2.12) can be obtained from (2.19) and (2.20) by formally setting $c_{02} = 0$ and $L \equiv 0$, the characters of the waves described by these two sets of equations are different. To see this note that if (α, t) are used as independent variables, (2.12) reduces to the simple condition

$$\partial H/\partial t = 0, \tag{2.29}$$

which integrates to give

$$H = H_0 + h(\alpha) \quad \text{where} \quad h(x) = H - H_0 \quad \text{at} \quad t = 0. \tag{2.30}$$

An immediate consequence of (2.30) is that any disturbance that is initially localized to the interval $-\lambda \leqslant x \leqslant 0$ is subsequently localized to the interval $-\lambda + c_0 t \leqslant x \leqslant c_0 t$. By contrast, when H satisfies (2.28) any initially localized disturbance immediately spreads to all parts of the x-axis.

Although there are many choices of $F(z)$ for which H and L remain bounded at all x for all $t \geqslant 0$, when $F(z)$ is determined so that H and L take *prescribed* values for all x at $t = 0$ then $F(z)$ is usually singular for some $t > 0$. In general, this either occurs for all x as $t \to \infty$, or at some finite value of t and x. To illustrate these two different kinds of instability note that when $h(x)$ and $L(x, 0)$, $= l(x)$ say, are analytic functions of the real variable x for *all* x, the solution to the Cauchy initial value problem for the elliptic equation (2.25) is given by (2.26) with

$$F(z) = h(z) + \mathrm{i}l(z). \tag{2.31}$$

The case when $l(x) \equiv 0$ is of special interest. Then, the first of equations (2.25) implies that condition (2.29) is satisfied at $t = 0$. This means that to an observer moving with the phase speed c_{01} the wave profile is not distorting at $t = 0$. With this choice of l it follows that

$$H = H_0 + \mathrm{Re}\,[h(z)]. \tag{2.32}$$

As an example of a disturbance that has an infinite amount of energy at $t = 0$ and which grows to become unbounded at all points as $t \to \infty$ consider the classical case when

$$h(x) = h_0 \cos 2\pi x/\lambda \quad \text{for} \quad -\infty \leqslant x \leqslant \infty. \tag{2.33}$$

Then, it follows from (2.32) that

$$H = H_0 + h_0 \cos(2\pi\bar{\alpha}) \cosh(2\pi\bar{t}), \tag{2.34}$$

where

$$\bar{\alpha} = \frac{\alpha}{\lambda} = \frac{x - c_{01} t}{\lambda} \quad \text{and} \quad \bar{t} = \frac{c_{02} t}{\lambda}. \tag{2.35}$$

Equation (2.34) describes a wave profile which moves with speed c_{01} wtihout distorting while at any fixed α its amplitude grows without bound as $t \to \infty$. By contrast, as an example of a disturbance that has infinite energy at $t = 0$ but which becomes unbounded at a single point at a finite time consider

$$h(x) = -h_0 \tanh(x/\lambda). \tag{2.36}$$

This profile and its subsequent development are depicted in figure 1*a*. The disturbance focuses and becomes unstable at $(\bar{\alpha}, |\bar{t}|) = (0, \frac{1}{2}\pi)$. This follows from the fact that when h is given by (2.36)

$$H = H_0 - h_0 \frac{\sinh 2\bar{\alpha}}{\cosh 2\bar{\alpha} + \cos 2\bar{t}}. \tag{2.37}$$

As an example of a disturbance that has a finite amount of energy at $t = 0$ and takes an infinite time to become unbounded at all x consider

$$h(x) = h_0 \exp[-x^2/\lambda^2]. \tag{2.38}$$

It then follows from (2.32) that

$$H = H_0 + h_0 \cos(2\bar{\alpha}\bar{t}) \exp[\bar{t}^2 - \bar{\alpha}^2]. \tag{2.39}$$

According to (2.39) the amplitude of the wave crest ($\bar{\alpha} = 0$) increases like $\exp[\bar{t}^2]$ while the free surface at a constant distance $|\alpha|$ from the crest oscillates with a local frequency $|c_{02}\alpha/\lambda|$ and an amplitude that also grows like $\exp[\bar{t}^2]$. The corresponding changes in the wave profile are shown in figure 1*b* for typical values of $\bar{t}$.

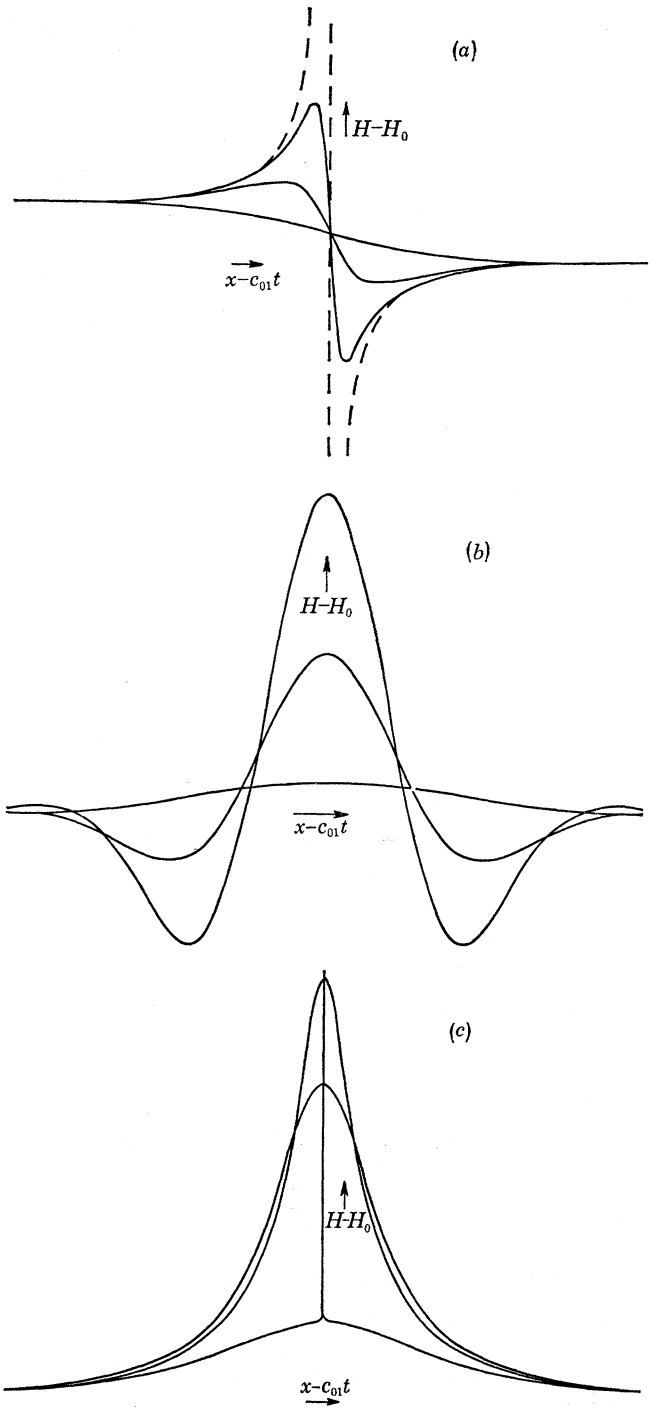

FIGURE 1. The changes of the wave profiles for three unstable disturbances as seen by an observer moving with speed c_{01}. (*a*) A disturbance that has an infinite amount of energy at $t = 0$ but which focuses and becomes unbounded at a definite point at a finite time. (*b*) A disturbance that has a finite amount of energy at $t = 0$ and becomes unbounded at all x as $t \to \infty$. (*c*) A disturbance that has a finite amount of energy at $t = 0$ and becomes unbounded at the wave crest at a finite time.

PHILOSOPHICAL TRANSACTIONS OF THE ROYAL SOCIETY A MATHEMATICAL, PHYSICAL & ENGINEERING SCIENCES

Finally, as an example of a disturbance that has a finite amount of energy at $t = 0$ and focuses to become unbounded at a single point take

$$h(x) = h_0 \lambda^2/(\lambda^2 + x^2). \tag{2.40}$$

It then follows that

$$H = H_0 + h_0 \frac{1 + \bar{\alpha}^2 - \bar{t}^2}{(1 + \bar{\alpha}^2 + \bar{t}^2)^2 - 4\bar{t}^2}. \tag{2.41}$$

This expression describes a disturbance that becomes unbounded at the wave crest $\bar{\alpha} = 0$ when $\bar{t} = 1$ (see figure 1*c*). This can be seen by noting that at the wave crest $\bar{\alpha} = 0$ (2.41) predicts that

$$H = H_0 + h_0(1 - \bar{t}^2)^{-1} \tag{2.42}$$

so that the amplitude of the crest is unbounded when $|\bar{t}| = 1$. On the other hand when $|\bar{t}| = 1$ and $\bar{\alpha} \neq 0$,

$$H = H_0 + h_0(4 + \bar{\alpha}^2)^{-1}. \tag{2.43}$$

Thus, at $(\bar{\alpha}, |\bar{t}|) = (0, 1)$ H is multivalued.

The general aim of this and subsequent studies is to show how the waves described above are modified by nonlinearity and viscous effects. In this paper we are mainly concerned with the effect of nonlinearity on neutrally stable disturbances on shear flows that contain a critical level where the wave velocity and the horizontal component of fluid velocity coincide. These waves contain trapped particles whose trajectories are generalizations of the famous Kelvin's cat's eyes. Now though, because of the effect of finite amplitude, these trajectories do not form closed orbits but distort as the particles are convected with the wave.

Although the terminology used in this paper is that associated with shallow-water gravity waves, the results obtained are directly applicable to many other hydraulic flows since the equations governing these flows can be transformed into the set (2.1)–(2.4) by replacing g by some function of H. This function is determined by the particular class of flows being analysed. Some of these flows, together with the appropriate transformations, are listed in § 10.

3. Shear flows with piecewise uniform vorticy

3.1. *Governing equations*

For the small amplitude waves described in § 2 the dependence of the flow variables on y can be computed independently of their dependence on (x, t). Although this decomposition is not usually possible for finite amplitude waves, there is a class of flows for which the dependence of the flow variables on y is immediately apparent and only their dependence on (x, t) must be calculated. These flows are characterized by the fact that the shear profile at some vertical cross-section, which is traversed by all particles in the flow, is always of the polygonal form shown in figure 2. It then follows that the flow consists of layers in each of which the vertical shear gradient,

$$\omega = \partial u/\partial y, \tag{3.1}$$

is constant. ω is the hydraulic flow approximation to the horizontal component of vorticity.

In this paper, in order to analyse the *broad* features of shear flows that contain a critical level, we consider the somewhat idealized situation when the flow consists of n layers in each of which ω is constant. These layers are separated by fluid interfaces that may also be vortex sheets across which the tangential component of fluid velocity is discontinuous. Although it might be thought that such an investigation would yield anomalous results at the critical level, as it automatically

assumes that $\partial^2 u/\partial y^2 = 0$ there, in a subsequent paper we show that during the passage of a large amplitude, neutrally stable disturbance the shear profile always adjusts so that $\partial^2 u/\partial y^2 = 0$ at the critical level.

To obtain the equations governing shear flows with piecewise uniform vorticity first note that when (2.1) is differentiated with respect to y, and (2.2) is used, it follows that ω is conserved at a particle so that

$$\frac{\mathrm{D}\omega}{\mathrm{D}t} = \frac{\partial \omega}{\partial t} + u\frac{\partial \omega}{\partial x} + v\frac{\partial \omega}{\partial y} = 0. \tag{3.2}$$

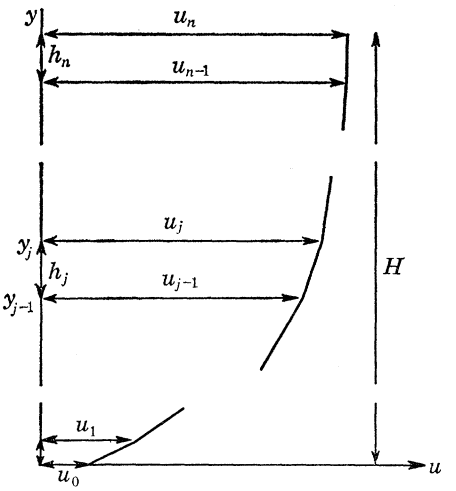

FIGURE 2. The n-layered polygonal shear profile on which the general analysis is based. The jth layer in which the uniform vorticity is ω_j is bounded by the curves $y = y_{j-1}(H)$ and $y = y_j(H)$ which are the images of particle paths in the (y, H) plane. The depth of this layer $h_j = y_j - y_{j-1}$.

An immediate consequence of (3.2) is that in any region spanned by particles that have crossed an interval of the y-axis where $\omega \equiv$ constant we can write

$$u = \omega y + \bar{u}(x, t). \tag{3.3}$$

It then follows from (2.2) that in this region

$$v = -y\,\partial\bar{u}/\partial x + \bar{v}(x, t). \tag{3.4}$$

When (3.3) and (3.4) are inserted in (2.1) this implies that

$$\frac{\partial \bar{u}}{\partial t} + \bar{u}\frac{\partial \bar{u}}{\partial x} + \omega\bar{v} + g\frac{\partial H}{\partial x} = 0. \tag{3.5}$$

If the flow consists of n layers, in each of which ω has a different value, the flow in each layer can be represented by relations such as (3.3)–(3.5) but now $\bar{u}$ and $\bar{v}$ differ from layer to layer. First we derive the conditions relating these variables when both u and v are continuous throughout the flow region and when ω is nowhere zero. Then, we show how these conditions must be modified when some of the interfaces separating the layers are vortex sheets and when $\omega = 0$ in some layers.

Let the interfaces $y = y_{j-1}(x, t)$ and $y = y_j(x, t)$ form the bottom and top of the jth layer in which the uniform vorticity in ω_j; then, in the jth layer we can write u in the form (3.3) with

$$\omega = \omega_j \quad \text{and} \quad \bar{u} = u_{j-1} - \omega_j y_{j-1} = u_j - \omega_j y_j \quad (j = 1, 2, \ldots, n), \tag{3.6}$$

where

$$u_j(x, t) = u \quad \text{at} \quad y = y_j(x, t) \quad (j = 0, 1, \ldots, n). \tag{3.7}$$

Also, v can be written in the form (3.4) with

$$\bar{v} = y_{j-1}\frac{\partial \bar{u}}{\partial x} + v_{j-1} = y_j \frac{\partial \bar{u}}{\partial x} + v_j \quad (j = 1, 2, \ldots, n), \tag{3.8}$$

where

$$v_j(x, t) = v \quad \text{at} \quad y = y_j(x, t) \quad (j = 0, 1, \ldots, n). \tag{3.9}$$

Since $y = y_j(x, t)$ is an interface, it also follows that

$$v_j = \frac{\partial y_j}{\partial t} + u_j \frac{\partial y_j}{\partial x} \quad (j = 0, 1, \ldots, n). \tag{3.10}$$

When the expressions (3.6) and (3.8) for $\bar{u}$ and $\bar{v}$ are inserted in (3.5) and condition (3.10) is used it follows that $u_j(x, t)$ satisfies the equation

$$\frac{\partial u_j}{\partial t} + u_j \frac{\partial u_j}{\partial x} + g\frac{\partial H}{\partial x} = 0 \quad (j = 0, 1, \ldots, n). \tag{3.11}$$

Note that

$$y_0 \equiv 0 \quad \text{and} \quad y_n = H(x, t) \tag{3.12}$$

and that (3.10) with $j = 0$ is equivalent to the boundary condition (2.3) while (3.10) with $j = n$ is equivalent to (2.4).

Equations (3.11) are $(n+1)$ relations between $(n+2)$ unknowns. To obtain the other relation note that (3.6) implies that the depth of the jth layer

$$h_j = y_j - y_{j-1} = \omega_j^{-1}(u_j - u_{j-1}) \quad (j = 1, 2, \ldots, n). \tag{3.13}$$

Consequently, since the total depth of the fluid layer is H, it follows that

$$H = \sum_{j=1}^{n} h_j = \sum_{j=1}^{n} \omega_j^{-1}(u_j - u_{j-1}). \tag{3.14}$$

Equations (3.11) and (3.14) form a complete set of $(n+2)$ equations for H and $(u_0, u_1, \ldots, u_n)$ as functions of (x, t). Once these variables have been calculated, conditions (3.13), and the fact that $y_0 = 0$, determine $(y_1, y_2, \ldots, y_{n-1})$ and then conditions (3.10) determine $(v_1, v_2, \ldots, v_n)$.

When some of the surfaces separating the layers are vortex sheets, (u_{j-1}, u_j) in (3.6) must be replaced by (u_{j-1}^+, u_j^-) where u_j^+ and u_j^- denote the limiting values of u as the surface $y = y_j$ is approached from above and below. Similarly, in (3.8) (v_{j-1}, v_j) must be replaced by (v_{j-1}^+, v_j^-). Also, condition (3.10) remains valid with (u_j, v_j) replaced either by (u_j^-, v_j^-) or by (u_j^+, v_j^+). It then follows that both u_j^+ and u_j^- satisfy (3.11) and that (u_j, u_{j-1}) in (3.14) must be replaced by (u_j^-, u_{j-1}^+).

When $\omega = 0$ in the jth layer, the formula (3.13) for h_j does not hold. Instead, h_j must be determined from the equation

$$\frac{\partial h_j}{\partial t} + \frac{\partial}{\partial x}(h_j u_j) = 0 \quad \text{where} \quad u_j = u_{j-1}. \tag{3.15}$$

To obtain these two conditions note that when $\omega_j \neq 0$ equations (3.11) imply that

$$\frac{\partial}{\partial t}[u_j - u_{j-1}] + \frac{1}{2}\frac{\partial}{\partial x}[(u_j + u_{j-1})(u_j - u_{j-1})] = 0, \tag{3.16}$$

or, by (3.13), that

$$\frac{\partial h_j}{\partial t} + \frac{1}{2}\frac{\partial}{\partial x}[(u_j + u_{j-1})h_j] = 0. \tag{3.17}$$

The results (3.15) follow directly from (3.13) and (3.18) in the limit as $\omega_j \to 0$ keeping h_j finite. When there are several layers in which $\omega = 0$ condition (3.14) must be modified to read

$$H = \sum_{\substack{\text{all layers} \\ \text{where } \omega \neq 0}} \omega_j^{-1}(u_j - u_{j-1}) + \sum_{\substack{\text{all layers} \\ \text{where } \omega = 0}} h_j. \tag{3.18}$$

In what follows, to simplify the discussion, we derive results for the case in which there are no vortex sheets and no layers in which $\omega = 0$. If necessary, the modifications that must be made when these conditions are not satisfied are simply quoted. They can usually be obtained by simple limiting procedures.

It should be noted that all of the equations derived above remain valid when g is replaced by an arbitrary function of H. Thus, the results described in this section are immediately applicable to the physical systems described in §10. However, since y is not usually a distance measure in a direction transverse to the main flow, as it is for shallow-water gravity waves, the procedure described in this section amounts to approximating the shear profile by a series of arcs whose shapes are determined by the particular system. For example, $y = \pi a^2$, for the axi-symmetric pipe flow described in §10.2 where a is the distance from the centre of the pipe, and the procedure is equivalent to approximating the shear profile by a series of parabolic arcs.

3.2. *Small amplitude disturbances*

Equations (3.11) and (3.14) have solutions describing steady parallel shear flows for which

$$H = H_0 \quad \text{and} \quad u_j = u_{0j} \quad (j = 0, 1, \ldots, n) \tag{3.19}$$

are constant. The only constraint on these constants is that they satisfy condition (3.14). When (3.11) and (3.14) are formally linearized about these solutions the resulting equations can be written

$$\frac{\partial u_j}{\partial t} + u_{0j}\frac{\partial u_j}{\partial x} + g\frac{\partial H}{\partial x} = 0 \quad (j = 0, 1, \ldots, n), \tag{3.20}$$

and

$$\sum_{j=1}^{n} \omega_j^{-1}(u_j - u_{j-1}) = H. \tag{3.21}$$

The solutions to these equations that are equivalent to the neutrally stable solutions (2.11) are given by

$$g(H - H_0) = \theta(x - c_0 t) \quad \text{and} \quad u_j = u_{0j} + \frac{\theta(x - c_0 t)}{c_0 - u_{0j}} \quad (j = 1, 0, \ldots, n), \tag{3.22}$$

where c_0 satisfies the characteristic condition

$$\sum_{j=1}^{n} \omega_j^{-1}\left[\frac{1}{c_0 - u_{0j}} - \frac{1}{c_0 - u_{0j-1}}\right] = g^{-1}. \tag{3.23}$$

The solutions that are equivalent to the unstable mode solutions (2.19) can be written

$$g(H - H_0) = \phi(x, t) \quad \text{and} \quad u_j = u_{0j} + \frac{[\mu - u_{0j}]\,\phi(x, t) - \eta\psi(x, t)}{[\mu - u_{0j}]^2 + \eta^2}, \tag{3.24}$$

where $c_0 = \mu + i\eta$ satisfies (3.23) while $\phi(x, t)$ and $\psi(x, t)$ satisfy the equations

$$\frac{\partial \phi}{\partial t} + \mu\frac{\partial \phi}{\partial x} = -\eta\frac{\partial \psi}{\partial x} \quad \text{and} \quad \frac{\partial \psi}{\partial t} + \mu\frac{\partial \psi}{\partial x} = \eta\frac{\partial \phi}{\partial x}. \tag{3.25}$$

With the u_j given by (3.22) or (3.24), the y_j can be calculated from (3.13) and the v_j from (3.10).

If it is assumed that the ω_j are different in adjacent layers, equation (3.23) can be regarded as an $(n+1)$th degree polynomial for all possible values of c_0. Generally, this polynomial has $(n+1)$ distinct roots, some real and some complex. The real roots correspond to neutrally stable modes, the complex roots to unstable modes. Any small amplitude disturbance can be regarded as a superposition of these non-interacting modes. For example, when there are $(n+1)$ real values, $(\lambda_1, \lambda_2, \ldots, \lambda_{n+1})$, of c_0 satisfying (3.23) any small amplitude disturbance can be represented in the form

$$g(H-H_0) = \sum_{r=1}^{n+1} \theta_r(x-\lambda_r t) \tag{3.26}$$

and

$$u_j = u_{0j} + \sum_{r=1}^{n+1} \frac{\theta_r(x-\lambda_r t)}{\lambda_r - u_{0j}} \quad (j = 0, 1, \ldots, n). \tag{3.27}$$

The $(n+1)$ functions $(\theta_1, \ldots, \theta_{n+1})$ can be chosen so that the $(n+1)$ functions $(u_0, u_1, \ldots, u_n)$ take prescribed values at $t = 0$. When (3.23) has m pairs of distinct complex roots

$$(\mu_1 \pm i\eta_1, \mu_2 \pm i\eta_2, \ldots, \mu_m \pm i\eta_m)$$

and $M = n+1-2m$ distinct real roots $(\lambda_1, \lambda_2, \ldots, \lambda_M)$, (3.25) and (3.26) must be modified to read

$$g(H-H_0) = \sum_{r=1}^{M} \theta_r(x-\lambda_r t) + \sum_{s=1}^{m} \phi_s(x,t) \tag{3.28}$$

and

$$u_j = u_{0j} + \sum_{r=1}^{M} \frac{\theta_r(x-\lambda_r t)}{\lambda_r - u_{0j}} + \sum_{s=1}^{m} \frac{[\mu_s - u_{0j}]\,\phi_s(x,t) - \eta_s \psi_s(x,t)}{[\mu_s - u_{0j}]^2 + \eta_s^2}; \tag{3.29}$$

the $\phi_s(x,t)$ and $\psi_s(x,t)$ satisfy the equations

$$\left.\begin{aligned} \frac{\partial \phi_s}{\partial t} + \mu_s \frac{\partial \phi_s}{\partial x} &= -\eta_s \frac{\partial \psi_s}{\partial x} \\ \text{and} \quad \frac{\partial \psi_s}{\partial t} + \mu_s \frac{\partial \psi_s}{\partial x} &= \eta_s \frac{\partial \phi_s}{\partial x}. \end{aligned}\right\} \quad s = 1, \ldots, m. \tag{3.30}$$

When the disturbance is of finite amplitude it cannot be regarded as a composite of non-interacting modes as it can in the small amplitude limit. Consequently, an analysis of the flow produced by a single finite amplitude mode is only of immediate physical relevance when it can be argued that this mode contains most of the energy of the disturbance. This occurs, for example, when the flow is stable and the disturbance is initially limited to a finite interval of the x-axis. Although the different neutrally stable modes interact for a time, ultimately, because they are moving at different speeds, they separate. Thus, at some later time the flow consists of isolated modes separated by regions of uniform parallel shear flow. With this interpretation in mind, in what follows we analyse the flow produced by a single finite amplitude neutrally stable mode. In the main we are concerned with critical modes that produce both subcritical and supercritical flow regions.

4. Large amplitude neutrally stable waves

4.1. *Polygonal profiles*

The finite amplitude generalizations of the neutrally stable waves are described by the simple wave solutions to equations (3.11) and (3.14). For these solutions we can write

$$u_j = U_j(H) \quad (j = 0, 1, \ldots, n), \tag{4.1}$$

where $H(x,t)$ satisfies the nonlinear progressing wave equation

$$\frac{\partial H}{\partial t}+c(H)\frac{\partial H}{\partial x}=0. \tag{4.2}$$

When the expressions (4.1) are inserted in (3.11) and (3.14), and the fact that H satisfies (4.2) is used, it follows that

$$\frac{\mathrm{d}U_j}{\mathrm{d}H}=\frac{g}{c-U_j} \quad (j=0,1,2,\ldots,n), \tag{4.3}$$

and that

$$\sum_{j=1}^{n}\omega_j^{-1}(U_j-U_{j-1})=H. \tag{4.4}$$

Conditions (4.3) and (4.4) provide $(n+2)$ equations for the $(n+2)$ variables $(U_0, U_1, \ldots, U_n; c)$ as functions of H. Then, the variation of H with (x,t) is determined from (4.2). A useful alternative to (4.4) is obtained by differentiating (4.4) with respect to H and then using (4.3) to eliminate the derivatives of the U_j. This yields the characteristic condition

$$\sum_{j=1}^{n}\omega_j^{-1}\left[\frac{1}{c-U_j}-\frac{1}{c-U_{j-1}}\right]=g^{-1}, \tag{4.5}$$

which can be viewed as an equation for $c(H)$ in terms of the shear profile at any vertical cross-section of the flow where the fluid depth is H.

Once $c(H)$ and the $U_j(H)$ have been determined, the images in the (y,H) plane of the stream-surfaces separating the layers are given by (3.13) as

$$y_j=Y_j(H)=\sum_{r=1}^{j}\omega_r^{-1}(U_r-U_{r-1}) \quad (j=0,1,\ldots,n). \tag{4.6}$$

It then follows from (3.10) and (4.2) that we can write

$$v_j=(\partial H/\partial x)\,V_j(H) \quad (j=0,1,\ldots,n), \tag{4.7}$$

where

$$V_j(H)=(U_j-c)\,\mathrm{d}Y_j/\mathrm{d}H. \tag{4.8}$$

When $\omega=0$ in some layers equation (4.4) must be replaced by (3.18) with $u_j=U_j(H)$. In these layers

$$\frac{\mathrm{d}h_j}{\mathrm{d}H}=g\frac{h_j}{(c-U_j)^2} \quad \text{and} \quad U_j=U_{j-1}. \tag{4.9}$$

These results follow directly from (3.15) when (4.2) and (4.3) are used. Also, (4.5), which is an alternative to (3.18), must be modified to read

$$\sum_{\substack{\text{all layers}\\ \text{where } \omega\neq 0}}\omega_j^{-1}\left[\frac{1}{c-U_j}-\frac{1}{c-U_{j-1}}\right]+\sum_{\substack{\text{all layers}\\ \text{where } \omega=0}}\frac{h_j}{(c-U_j)^2}=g^{-1}. \tag{4.10}$$

Note that equations (4.1)–(4.10) remain valid when g is replaced by any function of H. Thus, the above analysis is directly related to the flow listed in §10.

As a simple check on the above formula note that when the flow is unsheared, so that there is one layer in which $\omega=0$ and no layers in which $\omega\neq 0$, conditions (3.18) and (4.9) imply that

$$h_1=H \quad \text{and} \quad U_1-c=\pm(gH)^{\frac{1}{2}}. \tag{4.11}$$

Conditions (4.11) and (4.3) then imply that

$$U_1\pm 2(gH)^{\frac{1}{2}}=\text{constant}. \tag{4.12}$$

These are the well-known Riemann relations that hold for any progressing wave on an unsheared flow.

The finite amplitude waves described by (4.1)–(4.10) are neutrally stable disturbances in the sense that during their passage the total variations in H and in u at any fixed y are identical at all horizontal stations. These properties for H and u follow directly from (4.2) and (4.1). However, unlike the predictions of linear theory, the nonlinear theory predicts that the amplitude of v can grow as the wave propagates. For, when c varies with H, (4.2) predicts that the slope of the free surface will usually grow without bound in some part of the wave until, at some finite time, the wave breaks. When this occurs the hydraulic flow approximation, which is the basis of equations (2.1)–(2.4), is invalidated.

In general there is more than one set of variables $[U_0(H), U_1(H), \ldots, U_n(H)]$ satisfying equations (4.3) and (4.5) and taking prescribed values consistent with condition (4.4) at $H = H_0$. Equivalently, there is more than one finite amplitude neutrally stable mode for which the shear profile has a specified form at some cross-section of the flow where the depth is H_0. Each such mode can be characterized by the value of c_0, $= c(H_0)$, which satisfies (3.23) at $H = H_0$. c_0 is the velocity with which the depth $H = H_0$ propagates when only that mode is excited.

4.2. *General shear profiles*

Actually, although the analysis is much simpler for polygonal profiles, the equations governing finite amplitude neutrally stable waves can be found for quite general forms of the shear profile. This follows from a result first obtained by Blythe *et al.* (1972), who showed that equations (2.1)–(2.4) have solutions for which

$$u = U(H, y) \quad \text{and} \quad v = \frac{\partial H}{\partial x} V(H, y), \tag{4.13}$$

where $H(x, t)$ satisfies an equation of the form (4.2). When the forms (4.13) are inserted, and equation (4.2) is used, it follows from (2.1) and (2.2) that U, V and c satisfy the equations

$$(U-c)\frac{\partial U}{\partial H} + V\frac{\partial U}{\partial y} + g = 0 \tag{4.14}$$

and

$$\frac{\partial U}{\partial H} + \frac{\partial V}{\partial y} = 0. \tag{4.15}$$

In addition, conditions (2.3) and (2.4) imply that

$$V = 0 \quad \text{on} \quad y = 0 \tag{4.16}$$

while

$$V = U - c \quad \text{on} \quad y = H. \tag{4.17}$$

Equations (4.1)–(4.8) follow from (4.9)–(4.13) if it is assumed that U and V are piecewise linear functions of y.

The waves described by the solutions to equations (4.13)–(4.17) may be of infinite horizontal extent or they may be separated by sharp fronts from regions of parallel steady shear flow where $H \equiv$ constant and $v \equiv 0$ while u varies with y but not with x. This latter situation was discussed by Blythe *et al.* (1972) for the case when the flow was either wholly subcritical ($u < c$) or wholly supercritical ($u > c$). The simplest situation corresponds to a wave of constant length λ ($\gg H$) separating two semi-infinite regions where the flow is steady and parallel. When the flow is subcritical the shear profile $U_0(y)$ ahead of the wave, where $H = H_0$, can be specified since all particles in the wave have originated from this region. The speed c_0, with which this front

moves, satisfies (2.17). This follows directly from (4.14)–(4.17) by noting that (4.14) and (4.15) imply that

$$\frac{\partial}{\partial y}\left(\frac{V}{U-c}\right) = \frac{g}{(U-c)^2}. \tag{4.18}$$

When (4.18) is integrated between $y = 0$ and $y = H$ and the boundary conditions (4.16) and (4.17) are used it follows that

$$\text{at any fixed } H, \quad g\int_0^H \frac{\mathrm{d}y}{[U(H,y)-c]^2} = 1 \quad (U \neq c). \tag{4.19}$$

Condition (2.17) is a special case of (4.19) with $c = c_0$ and $U = U_0(y)$. For a polygonal shear profile which contains no level at which $U = c$, (4.19) integrates to give condition (4.5). (Note that in the jth layer $\mathrm{d}y = \omega_j^{-1}\mathrm{d}U$.) When the flow is supercritical the subscript zero refers to conditions behind the wave.

For flows containing a critical level at which $U = c$ the flow pattern is considerably more complex than it is when the flow is either wholly subcritical or wholly supercritical. Such waves usually contain trapped particles that are convected with the wave. Thus, in addition to specifying the vorticity ω at all particles in the subcritical flow region ahead of the wave and at all particles in the supercritical flow region behind the wave, ω must also be specified at all trapped particles. A further complication also arises from the fact that the speed of some of the particles that originated in the subcritical flow region ahead of the wave may increase after being overtaken by the wave so that, after spending a finite time in the wave, they are turned and exit at its front into the supercritical flow region. Similarly, some faster moving particles that enter the wave from behind can be slowed once they enter the wave so that, ultimately, they are overtaken by the wave. Thus, even though the disturbance can still be viewed as a region of unsteady flow separating two semi-infinite regions of steady parallel flow, the shear profile in the steady flow regions cannot be specified arbitrarily; if the particle that enters the wave at the level $y = Y_e$ exits at the level $y = Y_0$ then the vorticity at the levels $y = Y_e$ and $y = Y_0$ in the steady flow must be the same since ω is conserved at a particle. In general, this vorticity mixing process produces a shear profile that is inflectional at the critical level. The exceptional case is when the vorticity is the same at all particles that are turned by the wave. Then the vorticity mixing process produces a shear profile for which the vorticity is constant over some interval that includes the critical level. In what follows we consider a simple polygonal profile for which this condition is satisfied.

5. Two layered model

5.1. *Wave speeds*

Figure 3*a* shows a simple two-layered shear profile that can support a critical mode and for which there are no unstable modes. In the lower layer, of depth h ($= h_1$) the fluid has a uniform shear $\omega > 0$; in the upper layer the fluid is unsheared. It then follows that for neutrally stable waves we can write

$$u = \begin{cases} \omega y + U_0(H) & \text{for} \quad 0 \leqslant y \leqslant h(H), \\ U_1(H) & \text{for} \quad h(H) \leqslant y \leqslant H, \end{cases} \tag{5.1}$$

where

$$h = (U_1 - U_0)/\omega. \tag{5.2}$$

According to (4.3)

$$\frac{\mathrm{d}U_0}{\mathrm{d}H} = \frac{g}{c-U_0} \quad \text{and} \quad \frac{\mathrm{d}U_1}{\mathrm{d}H} = \frac{g}{c-U_1}. \tag{5.3}$$

PHILOSOPHICAL TRANSACTIONS OF THE ROYAL SOCIETY A MATHEMATICAL, PHYSICAL & ENGINEERING SCIENCES

Also,
$$[gH-(c-U_1)^2]\,(c-U_0) = g(U_1-U_0)^2/\omega. \tag{5.4}$$

This follows directly from (4.10) if we use the fact that the depth of the upper layer

$$h_2 = H-h = H-(U_1-U_0)/\omega. \tag{5.5}$$

Equations (5.3) and (5.4) govern the variations of $U_0(H)$, $U_1(H)$ and $c(H)$. Once these have been determined (5.2) and (5.5) determine $h(H)$. v can be determined either from the equations listed in §3.1 or, more directly, from (4.9), (4.11)–(4.13) and (5.1). These conditions imply that

$$v = \frac{\partial H}{\partial x}\begin{cases} g\dfrac{y}{U_0-c} & \text{for} \quad 0 \leqslant y \leqslant h \\ g\dfrac{y-H}{U_1-c}+U_1-c & \text{for} \quad h \leqslant y \leqslant H. \end{cases} \tag{5.6}$$

This variation is depicted in figure 3*b*.

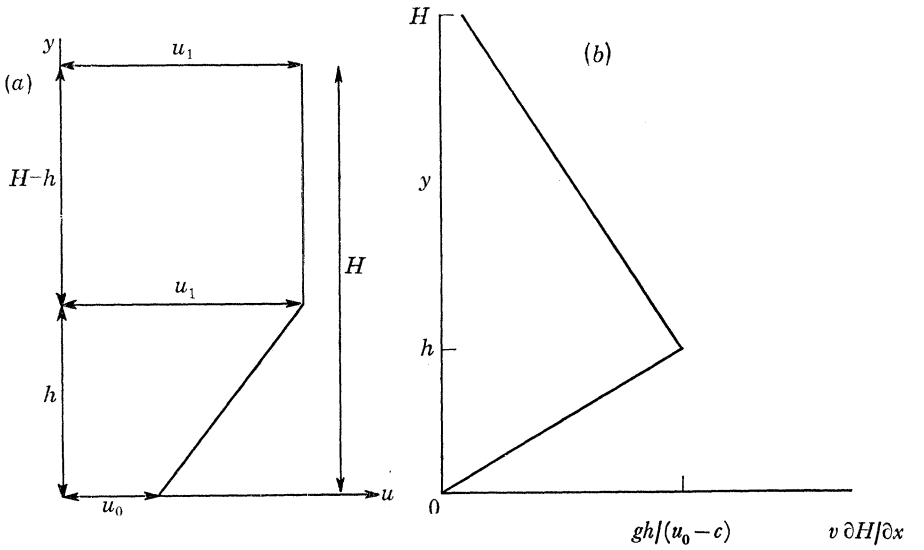

FIGURE 3. (*a*) A simple two-layered velocity profile which can support a critical mode. In the lower layer of depth h the vorticity, ω, is uniform. In the upper layer the fluid is unsheared. (*b*) The profile of the vertical component, v, of the fluid velocity when the horizontal component is as shown in figure 2*a*. The amplitude of v is proportional to $\partial H/\partial x$.

It is instructive to regard (5.4) as an equation for the normalized wave speed

$$c^* = \frac{c-U_0}{U_1-U_0} \tag{4.7}$$

as a function of
$$r = \frac{h}{H} = \frac{U_1-U_0}{\omega H} \quad \text{and} \quad F^2 = \frac{(U_1-U_0)^2}{gH}. \tag{5.8}$$

In terms of these variables (5.4) reads

$$\frac{c^*-r}{c^*(c^*-1)^2} = F^2. \tag{5.9}$$

For given values of r and the Froude number F there are three values of c^* satisfying (5.9) (see figure 4): one with $c^* < 0$, associated with a *backward* travelling wave; one with $c^* > 1$, associated with a *forward* travelling wave; and one with

$$0 \leqslant r \leqslant c^* \leqslant 1, \tag{5.10}$$

which is associated with a *slow* travelling wave. Since

$$U^* = \frac{U - U_0}{U_1 - U_0} \quad \text{lies in the range} \quad 0 \leqslant U^* \leqslant 1, \tag{5.11}$$

only the slow waves, for which $0 \leqslant c^* \leqslant 1$, are critical modes. For these waves (5.1), (5.7) and (5.8) imply that at the critical level where $u = c$

$$y = y_c(H) = c^* h \leqslant rh \leqslant h. \tag{5.12}$$

For the backward wave the flow is supercritical and for the forward wave it is subcritical.

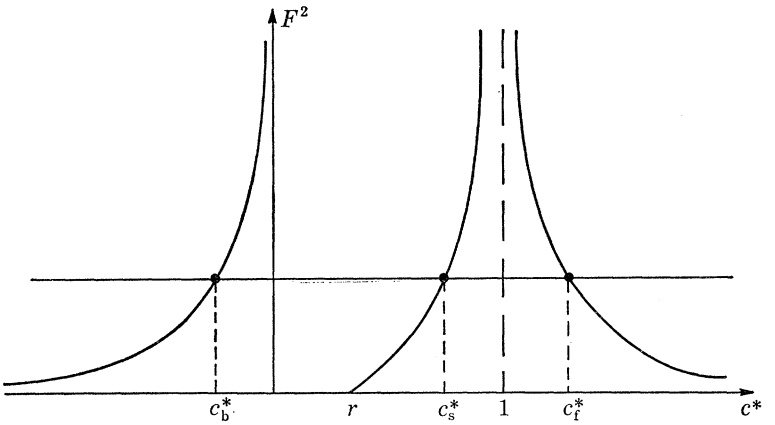

FIGURE 4. Depicts the variations of the three wave speeds as a function of F^2 at fixed r; c_b^*, c_f^* and c_s^* denote the speeds of the backward, forward and slow waves.

5.2. *Internal waves*

An analysis of all three families of waves is given in appendix A. For slow waves, which correspond to critical modes, all the solution curves of equations (5.3) and (5.4) pass through the singular point where

$$U_0 = U_1 = c \quad \text{and} \quad h = 0. \tag{5.13}$$

Any solution can be characterized by the value of $\omega^2 H_M/g$ where H_M, the value of H at which condition (5.13) holds, is the maximum value of H that can occur in the wave. In this and subsequent sections we discuss the special case as $\omega^2 H_M/g \to 0$. In this limit the critical modes are internal waves in the sense that although

$$H = H_M\left[1 + O\left(\frac{\omega^2 H_M}{g}\right)\right], \tag{5.14}$$

so that the free surface is essentially unperturbed during their passage, $r = h/H$ can vary over the full range $[0, 1]$.

If
$$c_M = c(H_M) \quad \text{and} \quad W = \omega H_M, \tag{5.15}$$

the solution to equations (5.3) and (5.4) in the limit as $\omega^2 H_M/g \to 0$ can be represented parametrically by the relations (see appendix A)

$$U_1 - c_M = \tfrac{1}{2} W r^2, \quad U_0 - c_M = W(\tfrac{1}{2} r - 1)\, r, \tag{5.16}$$

and
$$c - c_M = W(\tfrac{3}{2} r - 1)\, r, \tag{5.17}$$

where
$$H = H_M\left[1 + \frac{W^2}{g H_M}(\tfrac{1}{4} r - \tfrac{1}{3})\, r^3\right]. \tag{5.18}$$

Also, $$F^2 = \frac{W^2}{gH_M}r^2, \quad \leqslant \frac{W^2}{gH_M} = \frac{\omega^2 H_M}{g} \ll 1, \tag{5.19}$$

while the height of the critical level $$y_c = r^2 H_M. \tag{5.20}$$

We shall be concerned with waves of finite length λ separating two semi-infinite regions where the steady shear flows are identical and the fluid depth is H_∞. In view of (5.18), the internal wave limit corresponds to $\omega^2 H_\infty/g \ll 1$. Note that the constants c_M, H_M and W can be determined from the algebraic relations (5.15)–(5.18) in terms of $U_{0\infty}$, $U_{1\infty}$ and r_∞, the values of U_0, U_1 and r in the uniform flow.

It is convenient to measure all velocities in units of W, all vertical distances in units of H_M, all horizontal distances in units of λ and all times in units of λ/W. In terms of these units, the limiting form of the velocity field is given by the expressions

$$u = c_M + \begin{cases} y - r(1-\frac{1}{2}r) & \text{for} \quad 0 \leqslant y \leqslant r, \\ \frac{1}{2}r^2 & \text{for} \quad r \leqslant y \leqslant 1, \end{cases} \tag{5.21}$$

and

$$v = \frac{H_M}{\lambda}\frac{\partial r}{\partial x}\begin{cases} (1-r)y & \text{for} \quad 0 \leqslant y \leqslant r, \\ r(1-y) & \text{for} \quad r \leqslant y \leqslant 1. \end{cases} \tag{5.22}$$

Further, the pressure on $y = 0$,

$$p_0 = p_M + \rho W^2 r^3(\tfrac{1}{4}r - \tfrac{1}{3}). \tag{5.23}$$

The height of the interface separating the sheared from the unsheared flow is

$$y_i = r, \tag{5.24}$$

and the height of the critical level $$y_c = r^2. \tag{5.25}$$

In equations (5.21)–(5.25) $r(x, t)$ satisfies the equation

$$\frac{\partial r}{\partial t} + c(r)\frac{\partial r}{\partial x} = 0, \tag{5.26}$$

where $$c = c_M + r(\tfrac{3}{2}r - 1). \tag{5.27}$$

It follows from (5.23) that since p_0 is a monotonically decreasing function of r and that since $0 \leqslant r \leqslant 1$, p_0 can only vary in the range

$$p_M - \tfrac{1}{12}\rho W^2 \leqslant p_0 \leqslant p_M. \tag{5.28}$$

Consequently, the change in ground pressure during the passage of any of the waves is at most $\frac{1}{12}\rho W^2$. The variations of U_1, U_0 and c with p_0, which are calculated from (5.21), (5.23) and (5.27), are depicted in figures 5 and 6. Over the entire pressure range (5.28),

$$\frac{dU_0}{dp_0} > 0 \quad \text{and} \quad \frac{dU_1}{dp_0} < 0. \tag{5.29}$$

However, c does not vary monotonically with p_0:

$$\frac{dc}{dp_0} > 0 \quad \text{when} \quad 0 \leqslant \frac{p_M - p_0}{\frac{1}{2}\rho W^2} < \tfrac{1}{54} \quad (0 \leqslant r \leqslant \tfrac{1}{3}), \tag{5.30}$$

while

$$\frac{dc}{dp_0} < 0 \quad \text{when} \quad \tfrac{1}{54} < \frac{p_M - p_0}{\frac{1}{2}\rho W^2} \leqslant \tfrac{1}{6} \quad (\tfrac{1}{3} < r \leqslant 1). \tag{5.31}$$

Conditions (5.30) and (5.31), together with the fact that p_0 also satisfies equation (5.26), imply that large pressure gradients (which, by (5.22), produce large vertical currents) either form in that part of the wave where p_0 lies in the range (5.30) and is increasing at any fixed x during the passage of the wave, or where p_0 lies in the range (5.31) and is decreasing. In a subsequent paper we show how this property can be used to explain the formation of squall lines where large downdrafts form as the ground pressure drops and large updrafts form as the ground pressure increases. The associated phenomena for small amplitude waves is discussed in §8.

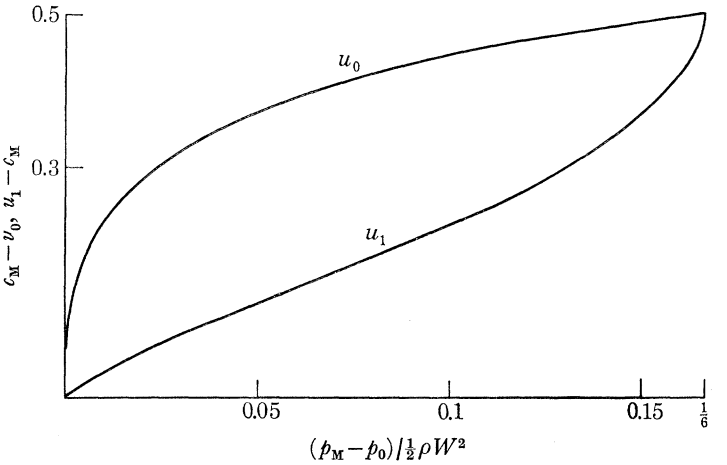

FIGURE 5. The variations of u_0 and u_1 with p_0 for internal waves.

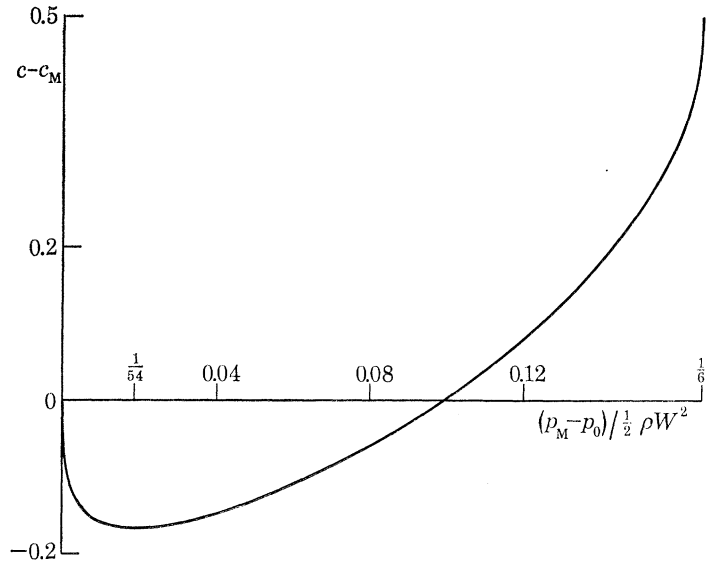

FIGURE 6. The variation of wave speed c with p_0 for internal waves.

For later use, it is convenient to have at hand a representation for $p_0(x, t)$. Suppose that at $t = 0$,

$$p_0 = \begin{cases} p_{0\infty} + \frac{1}{2}\rho W^2 \bar{p}(x) & \text{for} \quad -1 \leqslant x \leqslant 0, \\ p_{0\infty} & \text{elsewhere.} \end{cases} \tag{5.32}$$

The corresponding variation in r follows from condition (5.23): it is determined from the relation

$$\tfrac{1}{2}(r^4 - r_\infty^4) - \tfrac{2}{3}(r^3 - r_\infty^3) = \bar{p}(x) \quad \text{for} \quad -1 \leqslant x \leqslant 0, \tag{5.33}$$

where r_∞, the value of r outside the wave, satisfies the relation

$$\tfrac{1}{2}r_\infty^4 - \tfrac{2}{3}r_\infty^3 = \frac{p_{0\infty} - p_M}{\tfrac{1}{2}\rho W^2}. \tag{5.34}$$

Then, according to equations (5.26), (5.27), (5.23) and (5.33), at any subsequent time $p_0(x,t)$ and $r(x,t)$ inside the wave can be computed from the relations

$$\frac{p_0 - p_{0\infty}}{\tfrac{1}{2}\rho W^2} = \tfrac{1}{2}(r^4 - r_\infty^4) - \tfrac{2}{3}(r^3 - r_\infty^3) = \bar{p}(s) \quad (-1 \leqslant s \leqslant 0), \tag{5.35}$$

where $s(x,t)$ is determined from the equation

$$x - c_\infty t = s + (r - r_\infty)\left[\tfrac{3}{2}(r + r_\infty) - 1\right]t, \quad = d \quad \text{say.} \tag{5.36}$$

According to (5.27),

$$c_\infty = c_M + r_\infty(\tfrac{3}{2}r_\infty - 1). \tag{5.37}$$

6. Hydraulic channel flows

6.1. *An exact solution*

The velocity and pressure fields described by equations (5.21)–(5.28) are exact solutions of the equations

$$\frac{\partial u}{\partial x} + \frac{\partial v}{\partial y} = 0 \tag{6.1}$$

and

$$\frac{\partial u}{\partial t} + u\frac{\partial u}{\partial x} + v\frac{\partial u}{\partial y} + \frac{1}{\rho}\frac{\partial p_0}{\partial x} = 0 \quad \text{where} \quad p_0 = p_0(x,t). \tag{6.2}$$

These solutions also satisfy the conditions that

$$v = 0 \quad \text{on} \quad y = 0 \quad \text{and} \quad v = 0 \quad \text{on} \quad y = H_M. \tag{6.3}$$

Thus, the results of § 5.2, and the following analyses, are directly relevant to the study of unsteady hydraulic shear flows between two parallel flat plates. The plates could either be at $y = 0$ and at $y = H_M$, or at $y = 0$ and $y = 2H_M$ when the flow is symmetric about the centre plane $y = H_M$ (see figure 7). In fact, the solutions presented in § 5.2 are just a special case of a more general class of solutions to (6.1)–(6.3), that are valid for general shear profiles, for which

$$\frac{\partial p_0}{\partial t} + c(p_0)\frac{\partial p_0}{\partial x} = 0, \tag{6.4}$$

$$u = U(p_0, y) \quad \text{and} \quad v = \frac{\partial p_0}{\partial x}V(p_0, y) \tag{6.5}$$

while

$$V = 0 \quad \text{on} \quad y = 0 \quad \text{and} \quad V = 0 \quad \text{on} \quad y = H_M. \tag{6.6}$$

When the expressions (6.5) are inserted in (6.1) and (6.2), and (6.4) is used, if follows that

$$\frac{\partial U}{\partial p_0} + \frac{\partial V}{\partial y} = 0 \tag{6.7}$$

and that

$$(U - c)\frac{\partial U}{\partial p_0} + V\frac{\partial U}{\partial y} + \rho^{-1} = 0. \tag{6.8}$$

Unlike the situation when the flow has a free surface, the neutrally stable solutions described by (6.4)–(6.8) are only possible when the flow contains a critical level. This follows immediately from the fact that (6.7) and (6.8) imply that

$$\frac{\partial}{\partial y}\left(\frac{V}{U-c}\right) = \frac{1}{\rho(U-c)^2}. \tag{6.9}$$

Consequently, if there is no level at which $U = c$, (6.6) and (6.9) imply that

$$\int_0^{H_M} \frac{\mathrm{d}y}{(U-c)^2} = 0, \tag{6.10}$$

which is clearly impossible.

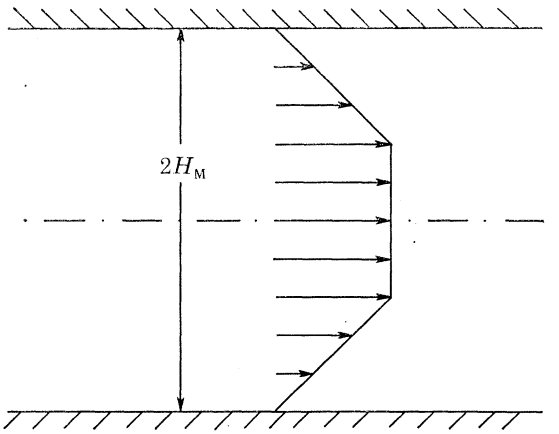

FIGURE 7. The shear profile assumed for the flow between two parallel flat plates discussed in section 6.

6.2. *Polygonal profiles*

Any polygonal shear profile also remains polygonal when the flow is governed by equations (6.1)–(6.3). The equations governing such flows are still those listed in section 3.1 except that the term $g\partial H/\partial x$ in equations (3.5) and (3.11) must be replaced by $\partial p_0/\rho\,\partial x$. Also, $H(x,t)$ in equations (3.12), (3.14) and (3.18) must be replaced by the constant H_M. The equations listed in section (3.2) still describe small amplitude disturbances if $g(H-H_0)$ in (3.22) and (3.24) is replaced by $(p_0-p_{00})/\rho$, where p_{00} is the constant pressure in the ambient flow, while H in (3.21) is replaced by H_M. Also, the constant g^{-1} in (3.23) must be replaced by zero.

For large-amplitude neutrally stable waves on flows with polygonal shear profiles equations (4.1) and (4.3) are replaced by the equations

$$u_j = U_j(p_0) \quad \text{and} \quad \frac{\mathrm{d}U_j}{\mathrm{d}p_0} = \frac{1}{\rho(c-U_j)} \tag{6.11}$$

while (4.5) becomes

$$\sum_{j=1}^{n} \omega_j^{-1}\left[\frac{1}{c-U_j} - \frac{1}{c-U_{j-1}}\right] = 0. \tag{6.12}$$

Note that whereas (4.5) was an $(n+1)$th degree polynomial for all possible values of c, (6.12) is an nth degree polynomial. Loosely, this is because the mode corresponding to a surface wave cannot be excited when the flow is contained between rigid boundaries.

The fact that the flow must contain a critical level can easily be deduced from (6.12). This condition can be written

$$\sum_{j=1}^{n} \frac{h_j}{(c-U_j)\,(c-U_{j-1})} = 0, \tag{6.13}$$

where $h_j = \omega_j^{-1}(U_j - U_{j-1})$ is the depth of the jth layer. In order to satisfy (6.13) there must be at least one layer in which $(c-U_j)\,(c-U_{j-1}) < 0$ and this is only possible if $c = U$ somewhere in the layer.

The general problem of finding necessary and sufficient conditions that must be satisfied for a flow with a free boundary to be approximated by a channel flow will not be discussed in any detail here. It seems clear though that a necessary condition is that the flow should contain a critical level because the approximating flow always does. The mathematical problem reduces to finding under what conditions the statement (4.5) can be approximated by the statement (6.12). It should be noted that (4.5) can be written as

$$\sum_{j=1}^{n} \pm F_j^{-2} = 1, \tag{6.14}$$

where

$$F_j = \left| \frac{(U_j - c)\,(U_{j-1} - c)}{g h_j} \right|^{\frac{1}{2}} \tag{6.15}$$

is the local Froude number of the jth layer. In (6.14) the plus sign corresponds to layers in which there is no critical level and the minus sign to (critical) layers in which there is. If there is one critical layer with Froude number F_c it follows from (6.14) that a sufficient condition for the flow to be approximated by a channel flow is that

$$F_c^2 \ll 1. \tag{6.16}$$

For the two-layered profile shown in figure 3*a*, (6.16) is a necessary and sufficient condition.

6.3. *The effect of an unsteady ambient pressure gradient*

Actually, with a slight reinterpretation of the variables the solutions presented in §5.2 are the most *general* solutions to equations (6.1)–(6.3) for which the shear profile is of the form shown in figure 3*a*. Physically, all hydraulic flows that are possible between two parallel flat plates which are consistent with this profile only differ from those described previously by the superposition of the effect of a time varying, but spatially uniform, pressure gradient.

To obtain this result note that in the lower layer where the vorticity is uniform

$$u = \omega y + u_0(x,t) \tag{6.17}$$

and, according to (6.1) and (6.3),

$$v = -y\,\partial u_0/\partial x. \tag{6.18}$$

When (6.17) and (6.18) are inserted, equation (6.2) implies that

$$\frac{\partial u_0}{\partial t} + u_0 \frac{\partial u_0}{\partial x} + \frac{1}{\rho}\frac{\partial p_0}{\partial x} = 0. \tag{6.19}$$

Also, in the unsheared upper layer equations (6.1)–(6.3) imply that

$$u = u_1(x,t) \quad \text{and} \quad v = (\partial u_1/\partial x)\,(H_M - y), \tag{6.20}$$

where

$$\frac{\partial u_1}{\partial t} + u_1 \frac{\partial u_1}{\partial x} + \frac{1}{\rho}\frac{\partial p_0}{\partial x} = 0. \tag{6.21}$$

Continuity of u and of v at the interface $y = H_M r(x,t)$ (6.22)

also imply that

$$r = (u_1 - u_0)/W \tag{6.23}$$

and

$$W r \frac{\partial r}{\partial x} = \frac{\partial u_1}{\partial x}. \tag{6.24}$$

From (6.23) and (6.24) $$u_0 = W(\tfrac{1}{2}r^2 - r) + c_{\mathrm{M}}(t) \tag{6.25}$$

and $$u_1 = \tfrac{1}{2}Wr^2 + c_{\mathrm{M}}(t), \tag{6.26}$$

where $c_{\mathrm{M}}(t)$ is an arbitrary function. When the expressions (6.25) and (6.26) for u_0 and u_1 are inserted in the equation obtained by eliminating $\partial p_0/\partial x$ from (6.19) and (6.21) it follows that $r(x, t)$ satisfies the equation

$$\partial r/\partial t + [c_{\mathrm{M}}(t) + W(\tfrac{2}{3}r^2 - r)]\,\partial r/\partial x = 0. \tag{6.27}$$

This integrates to give

$$r = \bar{r}(s) \quad \text{and} \quad x - x_\infty(t) = s + (r - r_\infty)\,[\tfrac{3}{2}(r + r_\infty) - 1]t, \tag{6.28}$$

where $$x_\infty(t) = \int_0^t c_\infty(t')\,\mathrm{d}t' \tag{6.29}$$

and $c_\infty(t)$ is given in terms of $c_{\mathrm{M}}(t)$ by (5.37).

It remains to calculate $p_0(x, t)$. This is done by using equations (6.19), (6.25) and (6.27): these yield

$$p_0 = p_{\mathrm{M}}(t) + \rho W^2(\tfrac{1}{4}r^4 - \tfrac{1}{3}r^3) - \rho(\mathrm{d}c_{\mathrm{M}}/\rho\mathrm{d}t)\,(x - x_\infty(t)), \tag{6.30}$$

where $p_{\mathrm{M}}(t)$ is an arbitrary function.

Except for the dependence of c_{M} and p_{M} on t, the general solutions obtained above are identical to those already constructed in §5.2. They can be used to describe a disturbance moving into a region where $H = H_\infty$ and, at any fixed (x, t), the shear profile is of the form depicted in figure 3*a*. However, the ambient flow has a time varying acceleration $\mathrm{d}c_{\mathrm{M}}/\mathrm{d}t$ that is balanced by a time varying, but spatially uniform, pressure gradient $-\rho\,\mathrm{d}c_{\mathrm{M}}/\mathrm{d}t$. *In a frame of reference moving with speed $c_{\mathrm{M}}(t)$ all these flows are identical when the pressure is computed relative to its ambient value.*

The effect of a time varying but spatially uniform ambient pressure gradient on the more general flows described by equations (2.1)–(2.4) can also be easily assessed. When p_{A}, the pressure on the free surface, is not uniform in x and t the right-hand side of (2.1) must be replaced by the 'body force' term $-\partial p_{\mathrm{A}}/\rho\,\partial x$. When this only varies with t, $= \mathrm{d}\Sigma(t)/\mathrm{d}t$ say, and the horizontal velocity profile in the constant depth region is of the form $u = \Sigma(t) + U_\infty(y)$, then the equations governing any disturbance are still of the form (2.1)–(2.3) but with x replaced by $x - \int^t \Sigma(t')\,\mathrm{d}t'$ and with u replaced by $u - \Sigma(t)$.

7. Particle paths

For neutrally stable waves with a free boundary it is possible to calculate the variation in the vertical height of any particle as a function of the current depth H independently of how H varies with (x, t). In fact the images in the (y, H) plane of any particle is an integral curve of the equation

$$\frac{\mathrm{D}y}{\mathrm{D}H} = \frac{V}{U - c}. \tag{7.1}$$

where $U(y, h)$, $V(y, H)$ and $c(H)$ satisfy equations (4.14)–(4.17). This follows directly from (4.13) and the fact that at any particle

$$\frac{\mathrm{D}y}{\mathrm{D}t} = v \quad \text{and} \quad \frac{\mathrm{D}H}{\mathrm{D}t} = \frac{\partial H}{\partial t} + u\frac{\partial H}{\partial x} = (U - c)\frac{\partial H}{\partial x}. \tag{7.2}$$

Similarly, for neutrally stable waves contained between rigid boundaries it is possible to calculate the variation in the vertical height of any particle as a function of p_0, the ground pressure

immediately below the particle, independently of how p_0 varies with (x, t). The images in the (y, p_0) plane of any particle is an integral curve of the equation

$$\frac{\mathrm{D}y}{\mathrm{D}p_0} = \frac{V}{U-c} \tag{7.3}$$

where $U(p_0, y)$, $V(p_0, y)$ and $c(p_0)$ satisfy equations (6.6)–(6.8).

For the two-layered profile, when the flow is described by equations (5.21)–(5.23), equation (7.3) implies that at any particle

$$\frac{\mathrm{D}y}{\mathrm{D}r} = \begin{cases} \dfrac{(1-r)\,y}{y-r^2} & \text{for} \quad 0 \leqslant y \leqslant r, \qquad (7.4) \\ \dfrac{1-y}{1-r} & \text{for} \quad r \leqslant y \leqslant 1, \qquad (7.5) \end{cases}$$

where

$$p_0 = p_{\mathrm{M}} + \rho W^2 r^3 (\tfrac{1}{4}r - \tfrac{1}{3}). \tag{7.6}$$

Several integral curves of the system (7.4)–(7.6) are depicted in figure 8. The arrows on these curves indicate the direction of particle motion in the part of the wave where $\partial p_0/\partial x > 0$. The direction of motion where $\partial p_0/\partial x < 0$ is obtained by reversing the directions of the arrows.

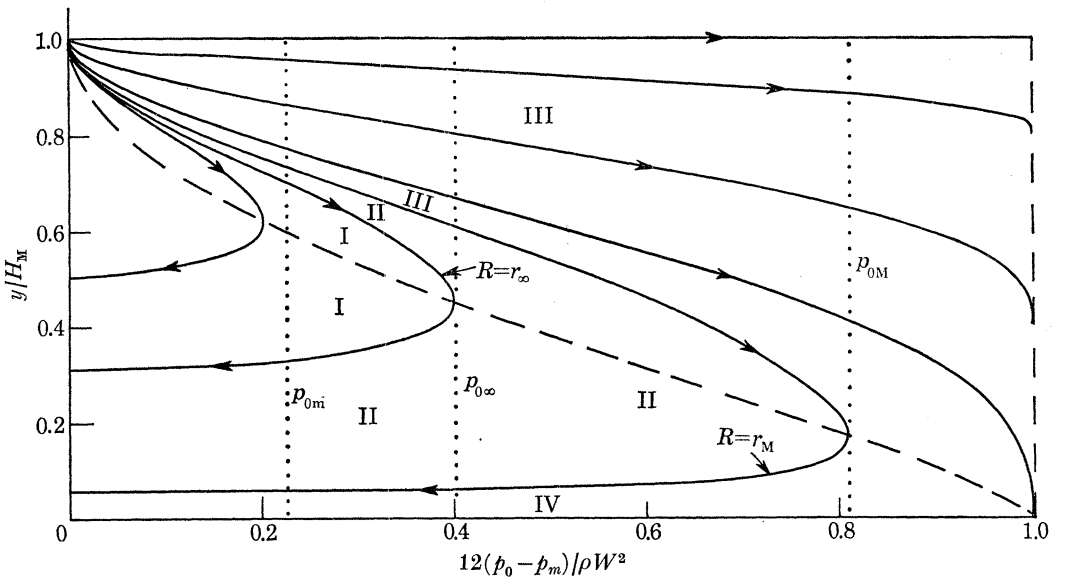

FIGURE 8. Particle trajectories in the (y, p_0) plane. Arrows denote the direction of travel in that part of the wave where $\partial p_0/\partial x > 0$. Where $\partial p_0/\partial x < 0$ reverse the arrows. – – –, the critical level. In an actual wave p_0 varies in some range $p_{0\mathrm{m}} \leqslant p_0 \leqslant p_{0\mathrm{M}}$. These levels, together with $p_{0\infty}$ the ground pressure outside the wave, are depicted by dotted lines. p_{M} and p_{m} are the extreme values of $p_{0\mathrm{M}}$ and $p_{0\mathrm{m}}$: $p_{\mathrm{M}} - p_{\mathrm{m}} = \frac{1}{12}\rho W^2$. The curves in region I are the trajectories of trapped particles. Those in II represent particles that leave the wave at the same side they entered but at a different height. Those in regions III and IV represent particles that completely traverse the wave.

An important integral curve of both (7.4) and (7.5) is

$$y = r, \quad = y_i. \tag{7.7}$$

This separates the lower region where the flow is sheared from the upper unsheared flow region. According to (7.6) and (7.7) the variation of y_i with p_0 is determined from the relation

$$\tfrac{1}{2}y_i^4 - \tfrac{2}{3}y_i^3 = (p_0 - p_{\mathrm{M}})/\tfrac{1}{2}\rho W^2. \tag{7.8}$$

Also shown in figure 8 is the variation in height of the critical level $y_c = r^2$. This is determined from the relation

$$\tfrac{1}{2}y_c^2 - \tfrac{2}{3}y_c^{\frac{3}{2}} = (p_0 - p_M)/\tfrac{1}{2}\rho W^2. \tag{7.9}$$

Both equations (7.4) and (7.5) can be integrated. The first can be transformed into a linear equation for r^{-1} as a function of y/r. This integrates to give

$$\frac{r-y}{y}\exp\left(\frac{1-r}{r-y}\right) = \text{constant}, \quad = \frac{1-R}{R}\exp(R^{-1}), \tag{7.10}$$

where the constant R, which can take any value in the range $[0, 1]$, labels the particle that crosses the critical level at $(r, y) = (R, R^2)$. In the vicinity of this level equation (7.10) implies that

$$y \simeq R^2 \pm R[2(1-R)(r-R)]^{\frac{1}{2}}, \tag{7.11}$$

so that a particle always moves in a direction of increasing r (decreasing p_0) after crossing the critical level. In practice, to compute the integral curves in the sheared flow it is best to express y and r as explicit functions of the variable $\sigma = y/r$ and of the parameter R, which is the value of σ at the critical level. Thus, relation (7.10) can be replaced by the two equivalent relations

$$r = \left[1 + (1-\sigma)\left(R^{-1} + \ln\frac{\sigma}{R}\frac{1-R}{1-\sigma}\right)\right]^{-1} \quad \text{and} \quad y = \sigma r(\sigma, R). \tag{7.12}$$

The branch of the integral curve above the critical level is obtained as σ varies in the range $R \leqslant \sigma \leqslant 1$. For the branch below σ varies over the range

$$[1 + (R^{-1} - 1)\exp(R^{-1})]^{-1} \leqslant \sigma \leqslant R. \tag{7.13}$$

Equation (7.5) easily integrates to give

$$(1-y) = (1-Y_0)(1-r), \tag{7.14}$$

where the parameter Y_0 labels the particles that intersect the curve $r = 0$ at $y = Y_0$.

In any particular wave p_0 will not, in general, vary over the full range (5.28) but only over some intermediate range

$$p_{0m} \leqslant p_0 \leqslant p_{0M}. \tag{7.15}$$

This corresponds to r varying over the range

$$r_m \leqslant r \leqslant r_M, \tag{7.16}$$

where r_m can be computed from p_{0M}, and r_M from p_{0m}, by relation (7.6). Consequently, only that part of figure 8 contained between the dotted lines $p_0 = p_{0m}$ and $p_0 = p_{0M}$ need be used to analyse the flow pattern. This can be divided into four non-overlapping regions. Region I, bounded by the line $p_0 = p_{0m}$ and the integral curve $R = r_\infty$; region II, bounded by the line $p_0 = p_{0m}$ and the integral curves $R = r_\infty$ and $R = r_m$, regions III and IV which are above and below region II. Particles (that are represented by integral curves) in region I are *trapped* particles. As they are convected with the wave they move up and down from subcritical to supercritical flow regions and back and forth inside the wave between adjacent equal pressure levels. The fact that they are trapped is easily deduced by noting that for a particle to enter or leave the wave it must attain a horizontal position, where $p_0 = p_{0\infty}$ $(r = r_\infty)$. None of the particles in region I do this. Particles in region II are of two kinds. Some enter the wave from behind at high supercritical levels but, before fully traversing the wave, are pulled below the critical level into the subcritical flow region where, because they are moving slower than the wave, they are subsequently overtaken by it. Other particles in region II enter the wave at its front at low subcritical levels and,

before being fully traversed by the wave, rise into the supercritical flow region where they move faster than the wave and finally exit at its front at a higher level than they entered. Finally, particles in region III enter the wave from behind at high supercritical levels, fully traverse it, and exit at its front at exactly the same level they entered, while particles in region IV enter at the front at low subcritical levels and, after being traversed by the wave, leave at the back at the same level they entered.

Note that when the wave is one of elevation only, so that $r_M = r_\infty$, there is no region I and, consequently, no particles are trapped in such a wave. On the other hand, when the wave is one of depression only ($r_m = r_\infty$) there is no region II so that all particles entering the wave at its front exit at its back, and all particles entering from the back exit at the front.

8. Kelvin's cat's eyes

8.1. *Large amplitude theory*

The actual trajectories of the particles in the (x, y) plane do, of course, depend on how p_0 varies with (x, t) or, equivalently, on the precise form of $\bar{p}(s)$. The trajectories of the trapped particles in region I are determined by relations of the form

$$y = \bar{y}(s; S), \quad x = \bar{x}(s; S) \quad \text{and} \quad t = \bar{t}(s; S), \tag{8.1}$$

where the parameter S identifies the particle that was at the critical level $(y, r) = (R^2, R)$ where $s = S$ at $t = 0$. R is determined as a function of S from the condition

$$R = \hat{r}(\bar{p}(S)), \quad \text{where} \quad r = \hat{r}(\bar{p}(s)) \tag{8.2}$$

is the solution to equation (5.35). The function $\bar{y}$ can be determined as a function of $\bar{p}(s)$ and $\bar{p}(S)$ from equations (7.10) and (8.2). To calculate the functions $\bar{x}$ and $\bar{t}$ use equation (5.36), which can be written

$$x = s + \bar{c}(s)\, t, \tag{8.3}$$

where $\bar{c}(s)$ is determined from equations (5.17) and (8.2), together with the fact that at any particle

$$\mathrm{D}x/\mathrm{D}t = u, \tag{8.4}$$

where u is given by the first of equations (5.21). When x, given by (8.3), is inserted in (8.4) it follows that the variation of t with s at any trapped particle satisfies the first order equation

$$(u - c)\frac{\mathrm{D}t}{\mathrm{D}s} - \frac{\mathrm{d}c}{\mathrm{d}s}t = 1. \tag{8.5}$$

It can be shown that this equation can be written

$$\mathrm{D}[\mathscr{A}(\bar{p}(s); \bar{p}(S))\, t]/\mathrm{D}s = \mathscr{B}(\bar{p}(s); \bar{p}(S)), \tag{8.6}$$

where

$$\mathscr{A} = \bar{y}(\hat{r} - \bar{y})^2 \quad \text{and} \quad \mathscr{B} = \bar{y}(\hat{r} - \bar{y})^2/(\bar{y} - \hat{r}^2). \tag{8.7}$$

It follows that at the particle 'S'

$$t = [\mathscr{A}(\bar{p}(s); \bar{p}(S))]^{-1} \int_S^s \mathscr{B}(\bar{p}(\theta); \bar{p}(S))\, \mathrm{d}\theta. \tag{8.8}$$

The function $\bar{x}$ is determined from (8.3) with t given by (8.8)

Although $\mathscr{B}$ is singular at $s = S$ where $y = r^2$, when $\bar{p}'(S) \neq 0$ the integral in (8.8) is finite. To see this first note that as $r \to R$ conditions (7.11) and (8.7) imply that

$$\mathscr{A} \to R^3(1 - R)^2 \quad \text{while} \quad \mathscr{B} \simeq \pm R^2(1 - R)^{\frac{3}{2}}[2(r - R)]^{-\frac{1}{2}}. \tag{8.9}$$

Then note that condition (5.35) implies that

$$\tfrac{1}{2}(r^4-R^4)-\tfrac{2}{3}(r^3-R^3)=\bar{p}(s)-\bar{p}(S), \tag{8.10}$$

so that
$$(r-R)\simeq[\bar{p}(S)-\bar{p}(s)]/2R^2(1-R) \quad \text{when} \quad |r-R|\ll R(1-R). \tag{8.11}$$

These conditions imply that when $|r-R|$ is small in the sense (8.11) the dominant approximation to t is

$$t\simeq\pm\int_S^s\frac{\mathrm{d}\theta}{(\bar{p}(S)-\bar{p}(\theta))^{\frac{1}{2}}}. \tag{8.12}$$

As particles always travel in a direction of decreasing p_0 (increasing r) after crossing the critical level, the term under the square root sign in (8.12) is positive. Hence, when particles cross in that part of the wave where $\mathrm{d}p_0/\mathrm{d}x>0$ ($\bar{p}'(s)>0$) they move in a direction of decreasing $x (s<S)$ and the minus sign must be taken in (8.12), while when they cross in the part of the wave where $\partial p_0/\partial x<0$ the plus sign must be taken. When (8.12) is inserted in (8.3), it follows that the dominant approximation to x in the vicinity of the critical level is

$$x\simeq s\pm\bar{c}(s)\int_S^s\frac{\mathrm{d}\theta}{(\bar{p}(S)-\bar{p}(\theta))^{\frac{1}{2}}}. \tag{8.13}$$

Finally, the dominant approximation to y is given by (7.11) and (8.11) as

$$y\simeq R^2\pm(\bar{p}(S)-\bar{p}(s))^{\frac{1}{2}}. \tag{8.14}$$

Particles at the critical level where $\bar{p}'(S)=0$ do not move relative to the wave but stay at $s=S$. Their trajectories are given by

$$x=S+\bar{c}(S)\,t \quad \text{and} \quad y=R^2. \tag{8.15}$$

According to figure 8, after crossing the critical level in a direction of decreasing $\bar{p}$ a particle either gains or loses height until it reaches a part of the wave where $\bar{p}'(s)=0$ and $\bar{p}''(s)>0$. Then, it reverses its vertical direction of travel until it again reaches the critical level at $s=S_1$ where

$$\bar{p}(S_1)=\bar{p}(S) \quad (S_1\neq S)$$

and
$$\bar{p}(s)<\bar{p}(S) \quad \text{for } s \text{ in the range } [s,S_1]. \tag{8.16}$$

The time it takes a particle to travel between these two adjacent identical pressure levels is, according to (8.8),

$$\tau(S)=[\mathscr{A}(\bar{p}(S);\bar{p}(S))]^{-1}\int_S^{S_1}\mathscr{B}(\bar{p}(\theta);\bar{p}(S))\,\mathrm{d}\theta. \tag{8.17}$$

After reaching $s=S_1$ the horizontal direction of travel of the particle relative to the wave is reversed until it again returns to $s=S$. During this return trip the statement (8.8) must be modified to read

$$t=[\mathscr{A}(\bar{p}(s);\bar{p}(S))]^{-1}\left[\mathscr{A}(\bar{p}(S);\bar{p}(S))\,\tau+\int_{S_1}^{S}\mathscr{B}(\bar{p}(\theta);\bar{p}(S))\,\mathrm{d}\theta\right]. \tag{8.18}$$

The time it takes to make this return transit between its two extreme horizontal positions (as viewed by an observer moving with the wave), as well as all subsequent transits, is always the same ($=\tau$). Moreover, since equal pressure levels propagate with equal speeds the horizontal distance between these two extreme positions remains unchanged as the particle moves back and forth in the wave. During the nth trip of the particle from $s=S$ to $s=S_1$, (8.8) must be modified to read

$$t=[\mathscr{A}(\bar{p}(s);\bar{p}(S))]^{-1}\left[\mathscr{A}(\bar{p}(S);\bar{p}(S))\,(n-1)\,\tau+\int_S^s\mathscr{B}(\bar{p}(\theta);\bar{p}(S))\,\mathrm{d}\theta\right]. \tag{8.19}$$

On the nth return trip from $s = S_1$ to $s = S$, (8.8) must be modified to read

$$t = [\mathscr{A}(\bar{p}(s);\bar{p}(S))]^{-1}\left[\mathscr{A}(\bar{p}(S);\bar{p}(S))\,n\tau + \int_{S_1}^{s}\mathscr{B}(\bar{p}(\theta);\bar{p}(S))\,\mathrm{d}\theta\right]. \tag{8.20}$$

In the vicinity of the critical level the dominant approximations to (8.19) and (8.20) are

$$t \simeq (n-1)\,\tau \pm \int_{S}^{s}\frac{\mathrm{d}\theta}{(\bar{p}(S)-\bar{p}(\theta))^{\frac{1}{2}}}, \tag{8.21}$$

and

$$t \simeq n\tau \pm \int_{S_1}^{s}\frac{\mathrm{d}\theta}{(\bar{p}(S)-\bar{p}(\theta))^{\frac{1}{2}}}. \tag{8.22}$$

It is usually convenient to plot the trajectory of a particle in terms of y and its horizontal position

$$d = x - c_\infty t \tag{8.23}$$

relative to the front rather than in terms of y and x. According to (8.3)

$$d = s + (\bar{c}(s) - c_\infty)\,t, \tag{8.24}$$

where t is given by (8.19) and (8.20). An immediate consequence of conditions (8.21)–(8.24) is that the trajectory of any particle trapped in the wave is not a closed orbit when viewed by an observer moving with the front, even though the horizontal distance between the extreme horizontal positions as well as the time it takes to travel this distance does not change for each particle. This is best seen by noting that D, the value of d at the extreme position S, varies with n according to the law

$$D = S + (\bar{c}(S) - c_\infty)\,\tau(S)\,(n-1), \tag{8.25}$$

while D_1, the value of d at the extreme position $S = S_1$, varies according to the law

$$D_1 = S_1 + (\bar{c}(S_1) - c_\infty)\,\tau(S_1)\,n. \tag{8.26}$$

As a particle crosses the critical level its direction of motion relative to an observer moving with speed c_∞ depends not only on the sign of $\bar{p}'(S)$ but also on whether r_∞ is less or greater than $\frac{1}{3}$. When $r_\infty < \frac{1}{3}$ particles at which

$$r_\infty < R < \tfrac{2}{3} - r_\infty \quad (c(S) < c_\infty) \tag{8.27}$$

move downwards and backwards relative to the front in the part of the wave where $\bar{p}'(S) > 0$ and upwards and forwards where $\bar{p}'(S) < 0$. However, particles at which $R > \frac{2}{3} - r_\infty$ move downwards and forwards where $\bar{p}'(S) > 0$ and upwards and backwards where $\bar{p}'(S) < 0$. When $r_\infty > \frac{1}{3}$ all particles move downwards and backwards where $\bar{p}'(S) > 0$ and upwards and forwards where $\bar{p}'(S) < 0$.

The trajectories of the particles in regions II, III and IV that traverse the region of constant shear but are not trapped are still governed by equations (7.4), (8.3) and (8.5). Now though it is convenient to label them by the time T and the height Y at which they enter the wave. In terms of these parameters the solution to (7.4) can be written

$$r = \left\{1 + (1-\sigma)\left[\frac{1-r_\infty}{r_\infty - Y} + \ln\left(\frac{r_\infty - Y}{Y}\,\frac{\sigma}{1-\sigma}\right)\right]\right\}^{-1}, \quad y = \sigma r(\sigma, Y). \tag{8.28}$$

The solution to (8.5) for the particles that enter from the front of the wave is

$$t = y^{-1}(r-y)^{-2}\left[Y(r_\infty - Y)^2 T + \int_0^s \frac{y(r-y)^2}{y-r^2}\,\mathrm{d}s\right]. \tag{8.29}$$

For those particles that enter the wave from behind the lower limit 0 in the integral must be replaced by -1.

For particles in region II, which do not fully traverse the wave since they never attain a position where $p_0 = p_M$, Y in equations (8.28) varies between the two roots Y_1 and Y_2 ($\leqslant Y_1$) of the transcendental equation

$$\frac{r_\infty - Y}{Y}\exp\left(\frac{1-r_\infty}{r_\infty - Y}\right) = (r_m^{-1} - 1)\exp(r_m^{-1}). \tag{8.30}$$

This is a special case of equations (8.28) with

$$R = \frac{r_\infty - Y}{1 - r_\infty} = r_m. \tag{8.31}$$

Note that in the special case when $r_m = 0$, $Y_1 = r_\infty$ and $Y_2 = 0$. Then, all particles that cross the front or the back where the flow is sheared cross the critical level and leave the wave at its front if they entered at the front and at the back if they entered at the back.

For particles in region III Y varies over the range $0 \leqslant Y \leqslant Y_2$, while in that part of region IV where the flow is sheared it varies over the range $Y_1 \leqslant Y \leqslant r_\infty$.

It remains to calculate the particle trajectories in the unsheared flow. All these enter the wave from behind. $y = \bar{y}(s; Y)$ can be determined immediately from (7.14) which implies that

$$1 - y = (1 - Y)(1 - r)/(1 - r_\infty), \tag{8.32}$$

where $r = \bar{r}(s)$ is given by (8.2). $\bar{x}(s; Y, T)$ and $\bar{t}(s; Y, T)$ are still determined from conditions (8.3) and (8.5). Now though u is given by the second of equations (5.21). When this expression is inserted, equation (8.5) integrates to give

$$t = r^{-1}(1-r)^{-2}\left[r_\infty(1-r_\infty)^2 T + \int_{-1}^{s}(1-r)\,\mathrm{d}s\right]. \tag{8.33}$$

8.2. *Small amplitude theory*

We illustrate the results obtained in the previous section by first considering small amplitude waves when $\bar{p}$ is small in the sense that

$$|\bar{p}| \ll r_\infty^3(1-r_\infty)^2. \tag{8.34}$$

Then, at the end of this section, these solutions are contrasted with a particular example of a large amplitude wave in which $|\bar{p}|$ varies over most of the maximum possible range

$$0 \leqslant |\bar{p}| \leqslant \tfrac{1}{6}. \tag{8.35}$$

In the small amplitude limit the vertical extent of the region containing trapped particles is vanishingly small, $O(|\bar{p}|^{\frac{1}{2}})$; in the large-amplitude limit it may span the whole fluid layer. However, even in the former limit nonlinear effects are important. They are of two kinds: those associated with the presence of a critical level, and those associated with the cumulative influence of amplitude dispersion.

When condition (8.34) holds, the appropriate approximations to r, u and v are

$$r = r_\infty - \tfrac{1}{2}r_\infty^{-2}(1-r_\infty)^{-1}\bar{p}(s); \tag{8.36}$$

$$u = u_{0\infty} + \begin{cases} y + \tfrac{1}{2}r_\infty^{-2}\bar{p}(s) & \text{for} \quad 0 \leqslant y \leqslant r, \quad (8.37) \\ r_\infty - \tfrac{1}{2}r_\infty^{-1}(1-r_\infty)^{-1}\bar{p}(s) & \text{for} \quad r \leqslant y \leqslant 1; \quad (8.38) \end{cases}$$

and

$$v = -\tfrac{1}{2}r_\infty^{-2}(1-r_\infty)^{-1}\frac{H_\infty}{\lambda}\bar{p}'(s)\frac{\partial s}{\partial x}\begin{cases} (1-r_\infty)\,y & \text{for} \quad 0 \leqslant y \leqslant r, \quad (8.39) \\ r_\infty(1-y) & \text{for} \quad r \leqslant y \leqslant 1. \quad (8.40) \end{cases}$$

In these equations $u_{0\infty}$ denotes the ground speed ahead of the wave and $s(d,t)$ is determined from the condition that

$$d = x - c_\infty t = s + \tfrac{1}{2} r_\infty^{-2}(1-r_\infty)^{-1}(1-3r_\infty)\,\bar{p}(s)\,t. \tag{8.41}$$

Also,

$$c_\infty = u_{0\infty} + r_\infty^2. \tag{8.42}$$

Note that, according to (8.41), when $r_\infty < \frac{1}{3}$ positive levels of $\bar{p}$ move faster than the wavefront, while when $r_\infty > \frac{1}{3}$ they move slower.

In the small amplitude limit the vertical displacements of particles crossing the critical level $y = y_c\,(\simeq r_\infty^2)$ is an order of magnitude higher than that of other particles. This is not because the magnitude of v is an order higher at the critical level than elsewhere but simply because these particles stay in the wave much longer. The precise form of the trajectories can easily be calculated from the limiting forms of equations (8.1)–(8.33) or directly from the velocity fields described by equations (8.36)–(8.42). For particles in region I they yield the expressions

$$y = r_\infty^2 \pm [\bar{p}(S) - \bar{p}(s)]^{\frac{1}{2}} \tag{8.43}$$

and

$$d = s + \tfrac{1}{2} r_\infty^{-2}(1-r_\infty)^{-1}(1-3r_\infty)\,\bar{p}(s) \begin{cases} (n-1)\,\tau \pm \displaystyle\int_S^s \frac{\mathrm{d}\theta}{(\bar{p}(S)-\bar{p}(\theta))^{\frac{1}{2}}}, & (8.44) \\ n\tau \pm \displaystyle\int_{S_1}^s \frac{\mathrm{d}\theta}{(\bar{p}(S)-\bar{p}(\theta))^{\frac{1}{2}}}, & (8.45) \end{cases}$$

for the trajectories. The arrival times are given by (8.21) and (8.22) with

$$\tau = \left| \int_S^{S_1} \frac{\mathrm{d}\theta}{(\bar{p}(S)-\bar{p}(\theta))^{\frac{1}{2}}} \right|. \tag{8.46}$$

The limiting forms of the particle trajectories in the other regions are easily calculated from equations (8.28)–(8.33), (8.36) and (8.41). In region II, which only occurs when $\bar{p} > 0$ in some part of the wave, the trajectories are described by (8.41) with

$$t = T \pm \int_0^s \frac{\mathrm{d}\theta}{[(Y-r_\infty^2)^2 - \bar{p}(\theta))]^{\frac{1}{2}}}, \quad (r_\infty^2 - \bar{p}_{\mathrm{M}}^{\frac{1}{2}} < Y < r_\infty^2), \tag{8.47}$$

for particles that enter the wave from the front and with

$$t = T \pm \int_{-1}^s \frac{\mathrm{d}\theta}{[(Y-r_\infty^2)^2 - \bar{p}(\theta]^{\frac{1}{2}}}, \quad (r_\infty^2 < Y < r_\infty^2 + \bar{p}_{\mathrm{M}}^{\frac{1}{2}}), \tag{8.48}$$

for those that enter from the back. In both cases

$$y = r_\infty^2 \pm [(Y-r_\infty^2)^2 - \bar{p}(s)]^{\frac{1}{2}}. \tag{8.49}$$

$\bar{p}_{\mathrm{M}}$ denotes the maximum value of $\bar{p}$ in the wave.

In region IV and that part of region III where the flow is sheared d is again given by (8.41) with t given by (8.47) for $0 \leqslant Y \leqslant r_\infty^2 - \bar{p}_{\mathrm{M}}^{\frac{1}{2}}$ and by (8.48) for $r_\infty^2 + \bar{p}_{\mathrm{M}}^{\frac{1}{2}} \leqslant Y \leqslant r_\infty$. However, y must be determined from the condition

$$\frac{r_\infty^2}{Y^2}\left(\frac{Y-r_\infty}{1-r_\infty}\right)^2 (y-Y)^2 + 2r_\infty^2 \frac{Y-r_\infty^2}{Y}(y-Y) + \bar{p} = 0. \tag{8.50}$$

This can be obtained from equations (7.12), or, more directly, by using (7.4) to expand $(r-r_\infty)$ as a power series in $(y-Y)$ and then using (8.36) to express $(r-r_\infty)$ in terms of $\bar{p}$. The statement (8.50) is uniformly valid in the shear flow region at all particles that are not trapped. Actually,

without loss in accuracy, the coefficient of $(y-Y)^2$ can be replaced by unity, its value at the critical level where $Y \simeq r_\infty^2$. When $|Y-r_\infty^2| \gg |\bar{p}|^{\frac{1}{2}}$ the statement (8.50) is well approximated by

$$y = Y - \frac{1}{2}\frac{Y}{r_\infty^2(Y-r_\infty^2)}\bar{p}(s). \tag{8.51}$$

Then,
$$t = T + (Y-r_\infty^2)^{-1}s \quad (0 \leqslant Y \leqslant r_\infty^2 - \bar{p}_{\mathrm{M}}^{\frac{1}{2}}), \tag{8.52}$$

for the particles that enter the wave at its front while

$$t = T + (Y-r_\infty^2)^{-1}(1+s) \quad (r_\infty^2 + \bar{p}_{\mathrm{M}}^{\frac{1}{2}} \ll Y < r_\infty), \tag{8.53}$$

for those that enter at the back.

Finally, in the part of region III where the flow is unsheared d is given by (8.41) with

$$t = T + \frac{(s+1)}{r_\infty(1-r_\infty)} \tag{8.54}$$

while
$$y = Y - \frac{1}{2}\frac{(1-Y)}{r_\infty^2(1-r_\infty)^2}\bar{p}(s). \tag{8.55}$$

According to (8.41) the effect of amplitude dispersion can only be neglected when

$$t \ll 2\frac{r_\infty^2(1-r_\infty)}{|1-3r_\infty|\,|\bar{p}'(s)|_{\max}}, \quad = t_{\mathrm{B}} \quad \text{say.} \tag{8.56}$$

For these times s can be formally approximated by d in equations (8.43), (8.46) and (8.47)–(8.55). In particular, equation (8.43) then yields the simple explicit expression

$$y = r_\infty^2 \pm [\bar{p}(S) - \bar{p}(d)]^{\frac{1}{2}} \tag{8.57}$$

for the trajectories of the trapped particles in the (y, d) plane. This relation describes the classical Kelvin cat's eye pattern for the particle paths which, to the approximation that amplitude dispersion is not important, form closed curves that do not distort as the particles move backwards and forwards in the wave. However, when condition (8.56) does not hold the parameter s cannot be approximated by d and the full equations (8.48)–(8.46) must be used to calculate the particle trajectories. Ultimately, of course, the wave usually breaks. When $r_\infty < \frac{1}{3}$ this first occurs at $t = t_{\mathrm{B}}$ in a part of the wave where $\bar{p}'(s) < 0$, which means that breaking occurs when the pressure is rising during the passage of the wave. This is the usual situation in hydraulics. However, when $r_\infty > \frac{1}{3}$ breaking first occurs at $t = t_{\mathrm{B}}$ where $\bar{p}'(s) > 0$, or in a part of the wave where the pressure is falling during the passage of the wave! The effect of breaking will not be analysed here.

The fact that the vertical displacements of the particles in the vicinity of the critical level are an order of magnitude higher than elsewhere follows immediately from (8.43) and (8.53). At the critical level they are $O(|\bar{p}|^{\frac{1}{2}})$, in the unsheared flow they are $O(|\bar{p}|)$. This is well illustrated in figures 9 and 10 which depict typical particle trajectories in the vicinity of the critical level when

$$\bar{p}(x) = -\epsilon \sin^2 \pi x \quad (-1 \leqslant x \leqslant 0,\ \epsilon > 0). \tag{8.58}$$

For such waves
$$t_{\mathrm{B}} = \frac{2}{\pi}r_\infty^2(1-r_\infty)\,|1-3r_\infty|^{-1}\epsilon^{-1} \tag{8.59}$$

and breaking always occurs at $d = -0.09$ when $r_\infty > \frac{1}{3}$ and at $d = -0.91$ when $r_\infty < \frac{1}{3}$. Only trajectories in the vicinity of the critical level are shown and the vertical scale measure is $(y-r_\infty^2)/\epsilon^{\frac{1}{2}}$. On this scale the particle trajectories away from the critical level are horizontal. For the situation

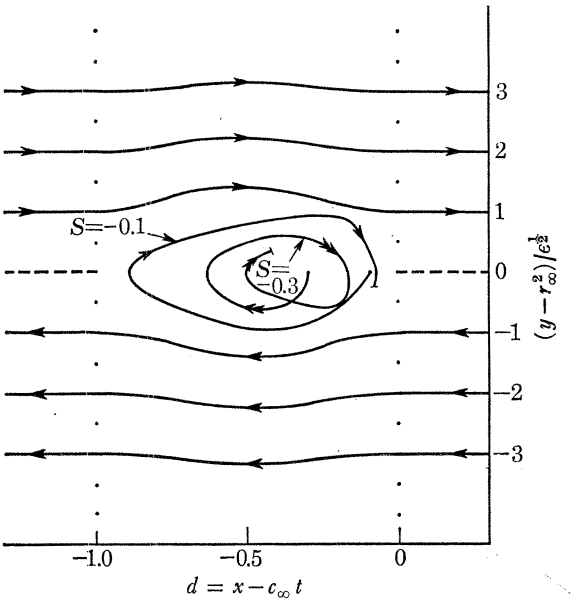

FIGURE 9. Particle trajectories as viewed by an observer moving with the front in a small amplitude wave. At $t = 0$, $\bar{p} = -\epsilon \sin^2 \pi x$, where $\epsilon = 2 \times 10^{-5}$. Since $r_\infty^2 = 0.9 > \frac{1}{9}$, $\mathrm{d}c/\mathrm{d}p_0 < 0$ and the wave steepens at the front where the pressure is falling. It breaks at $t_B = 796$. Only trajectories in the vicinity of the critical level are shown and the vertical scale measure is $\epsilon^{-\frac{1}{2}}(y - r_\infty^2)$. Away from this level the flow remains essentially parallel. The trajectories of the two trapped particles $S = -0.1$ and $S = -0.3$ are shown. The wave breaks before these have made two complete orbits: the Kelvin's cat's eye pattern rapidly distorts.

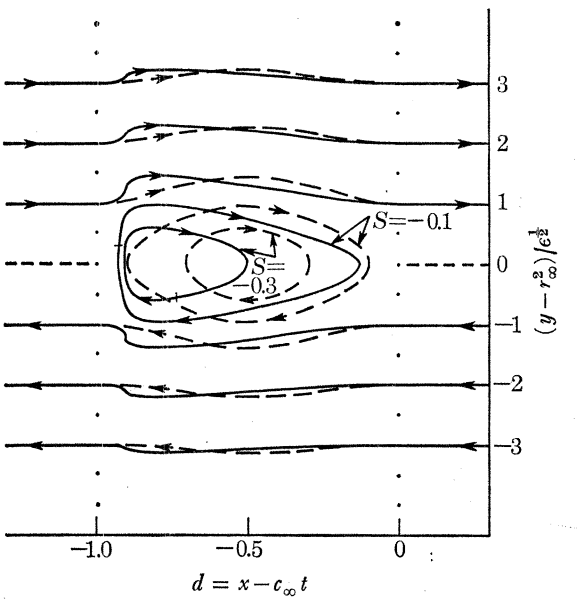

FIGURE 10. Particle trajectories as viewed by an observer moving with the front in a small amplitude wave. At $t = 0$ $\bar{p} = -\epsilon \sin^2 \pi x$ where $\epsilon = 10^{-4}$. Now, since $r_\infty^2 = 0.1 < \frac{1}{9}$, $\mathrm{d}c/\mathrm{d}p_0 > 0$ and the wave steepens at the back where the pressure is rising. It breaks at $t_B = 8483$. The trapped particles $S = -0.1$ and $S = -0.3$ make 25 and 38 orbits before breaking occurs. Since $|\mathrm{d}c/\mathrm{d}p_0|$ is much smaller than for the situation depicted in figure 9 the cat's eye pattern distorts slower. The broken curves denote the particle trajectories during the first orbits, the full curves just prior to breaking. Also shown are typical trajectories of particles that enter the wave and completely traverse it. The broken curves represent particles that enter at $t = 0$ and the full curves particles that enter at the same height at $t = t_B$.

depicted in figure 9, $r_\infty^2 = 0.9$ and $\epsilon = 2 \times 10^{-5}$, which yields $t_B \simeq 796$. The trajectories of the two trapped particles $S = -0.1$ and $S = -0.3$ are shown. Since $\tau(-0.1) \simeq 371$ and $\tau(-0.3) \simeq 248$ neither of these particles complete more than one complete orbit before the wave breaks. Thus, even though the small amplitude requirement (8.34) is satisfied, the effect of amplitude dispersion is significant before these particles make one complete orbit. Figure 10 depicts the situation when $r_\infty^2 = 0.1$ and $\epsilon = 10^{-4}$ to yield $t_B \simeq 8483$. Now $\tau(-0.1) \simeq 166$ and $\tau(-0.3) \simeq 111$ so that the trapped particles $S = -0.1$ and $S = -0.3$ make 25 and 38 circuits respectively before the wave breaks. The broken curves depict either the first orbits of these trapped particles or the paths of particles that enter the wave at $t = 0$. The full curves depict either the last orbits of the same trapped particles or the paths of particles that enter the wave just before it breaks.

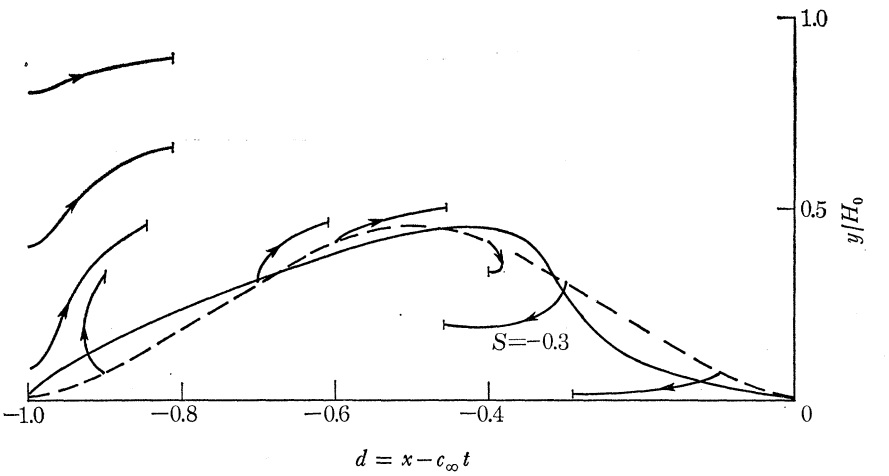

FIGURE 11. Typical particle trajectories in a large amplitude wave for which $\bar{p} = -0.1 \sin^2 \pi s$ and $r_\infty^2 = 10^{-2}$. The wave amplitude is sufficiently large for dc/dp_0 to be positive in some parts of the wave and negative in others. Thus, steepening occurs in a part of the wave where the pressure is dropping and also in a part where the pressure is rising. (See figure 15 and the accompanying caption.) The broken curve depicts the position of the critical level at $t = 0$ and the full curve (without arrows) its position just prior to breaking which first occurs at the front at $t = 1.35$. The full curves with arrows are the trajectories of some typical particles for $0 \leqslant t \leqslant 1.35$.

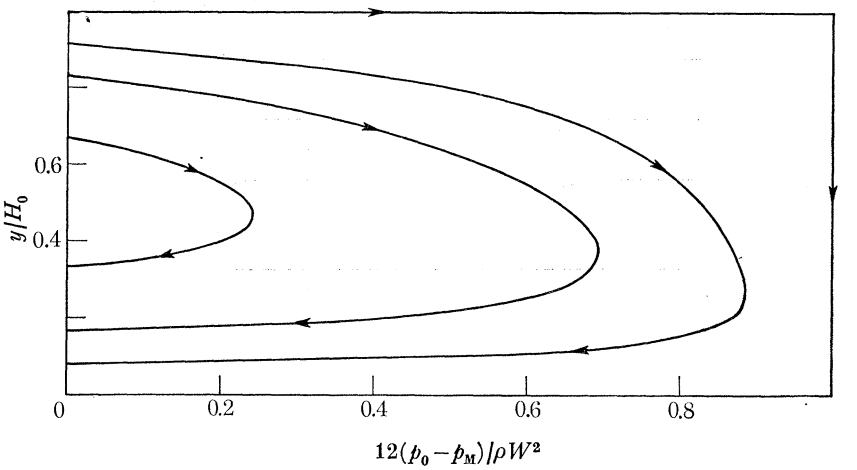

FIGURE 12. Streamline pattern in the (y, p_0) plane as viewed by an observer moving with speed c_M. This pattern is independent of $p_0(x, t)$ except that the arrows indicate the flow directions in the part of the wave where $\partial p_0/\partial x > 0$.

Figure 12 depicts typical particle paths when $r_\infty^2 = 10^{-2}$ and $\epsilon = 10^{-1}$. For these values of the parameters the wave associated with the pressure variation (8.58) is a large amplitude wave and the full equations listed in section 8 must be used to calculate the flow variables. The wave breaks at $t \simeq 1.35$. Only the paths of particles up until this time are shown. None of the particles that crossed the critical level at $t = 0$ (depicted by the broken curve) have made a complete orbit before the wave breaks, neither have the particles that entered the wave from the back yet fully traversed the wave.

9. Streamlines

The images of the streamlines in the (y, p_0) plane can also be determined independently of how p_0 varies with (x, t). To do this note that the streamline pattern relative to an observer moving with a horizontal velocity q is determined from the condition that

$$\frac{\mathrm{d}y}{\mathrm{d}x} = \frac{v}{u-q}. \tag{9.1}$$

When the expressions (5.21) and (5.22) for u and v are inserted in (9.1) it follows that the images of the streamlines in the (y, r) plane can be calculated from the conditions that

$$\frac{\mathrm{d}y}{\mathrm{d}r} = \begin{cases} (1-r)\,y/(y+\frac{1}{2}r^2-r-\bar{q}) & \text{for} \quad 0 \leqslant y \leqslant r, \\ r(1-y)/(\frac{1}{2}r^2-\bar{q}) & \text{for} \quad r \leqslant y \leqslant 1. \end{cases} \tag{9.2}$$

The constant $$\bar{q} = (q - c_{\mathrm{M}})/W \text{ (in dimensional variables).} \tag{9.3}$$

In particular, when $q = c_\infty$ $$\bar{q} = \tfrac{3}{2}r_\infty^2 - r_\infty. \tag{9.4}$$

Equations (9.2) integrate to give

$$r = \begin{cases} 1-[1+2\bar{q}-y-\bar{y}^2y^{-1}]^{\frac{1}{2}} & \text{for} \quad 0 \leqslant y \leqslant r, \\ \left(\dfrac{\bar{y}^2-2\bar{q}y}{1-y}\right)^{\frac{1}{2}} & \text{for} \quad r \leqslant y \leqslant 1. \end{cases} \tag{9.5}$$

The parameter $\bar{y}$, which is constant at a streamline, can take any value in the range $(0, \bar{q}+\frac{1}{2})$. The variation of y with p_0 at any streamline can now be calculated from (9.5) and (5.11). This is illustrated in figure 12 when $q = c_{\mathrm{M}}$ $(\bar{q} = 0)$.

Figures 13 and 14 depict typical streamline patterns as seen by an observer moving with the front speed c_∞ when the particle paths are those shown in figures 9 and 10. The broken curves denote the streamlines at $t = 0$ and the full curves at an instant just before breaking occurs. The ground-pressure signatures at these times are also shown. Note that although the effect of unsteadiness is insignificant over the time that it takes a particle to make one complete orbit when $(r_\infty^2, \epsilon) = (10^{-1}, 10^{-4})$ (particle paths and streamlines almost coincide), the effect of unsteadiness is clearly significant over this time when $(r_\infty^2, \epsilon) = (0.9, 2 \times 10^{-5})$. Of course, even in the former case the cumulative effect of unsteadiness has completely changed the pattern before breaking occurs.

Figure 15 shows the change in the streamline pattern and ground pressure signature in the large amplitude wave whose particle paths are shown in figure 11. Note that the pressure profile steepens towards the front of the wave where the pressure is falling and also towards the back where the pressure is rising. This produces large downdrafts towards the front and large updrafts towards the back of the wave. The explanation easily follows from the graph for $c(p_0)$ (see figure 6). Since $r_\infty < \frac{1}{3}$, as p_0 drops from $p_{0\infty}$ to $(p_0)_{\mathrm{crit}}$ (at which $r = \frac{1}{3}$) c decreases and the wave flattens.

Then, any further decrease in p_0 is accompanied by an increase in c so that over this pressure range the wave steepens as p_0 falls. After p_0 has reached its minimum value and begins to rise c at first decreases and the wave flattens. However, after p_0 has passed $(p_0)_{\text{crit}}$ on its way back to $p_{0\infty}$ c again begins to increase and the wave steepens as p_0 rises.

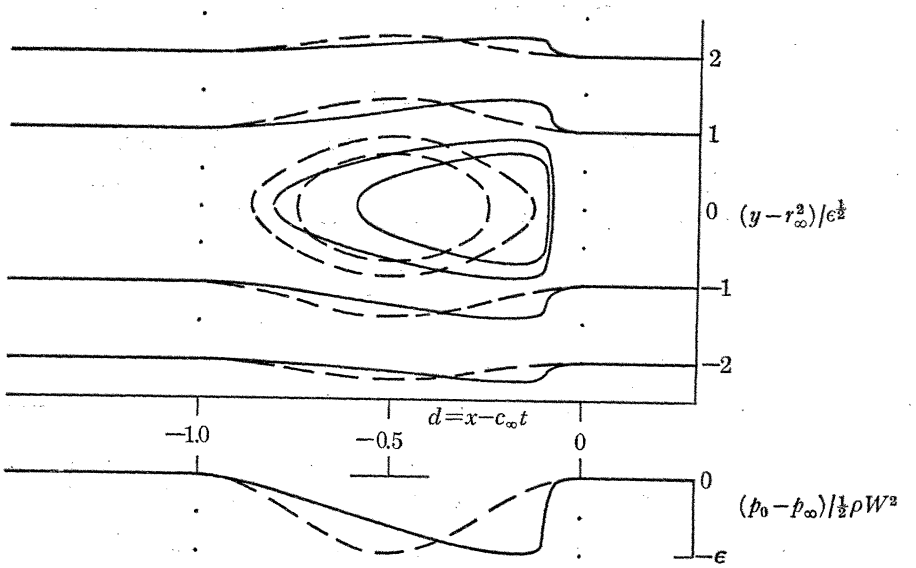

FIGURE 13. The ground pressure signature and typical instantaneous streamline patterns (flow directions) as viewed by an observer moving with speed c_∞ when the particle trajectories are those shown in figure 9. – – –, The situation at $t = 0$; ——, the situation at $t = t_B$. Since $dc/dp_0 < 0$ everywhere breaking only occurs at $d = -0.09$ where p_0 is dropping.

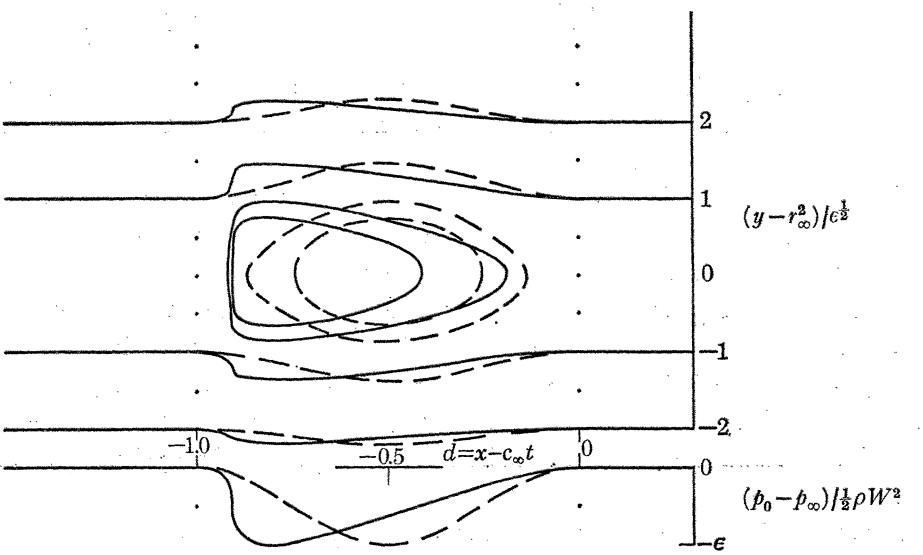

FIGURE 14. The ground pressure signature and typical streamline patterns as viewed by an observer moving with speed c_∞ when the particle trajectories are those shown in figure 10. – – –, The situation at $t = 0$; ——, the situation at $t = t_B$. Now, since $dc/dp_0 > 0$ everywhere breaking only occurs at $d = -0.91$, where the pressure is rising.

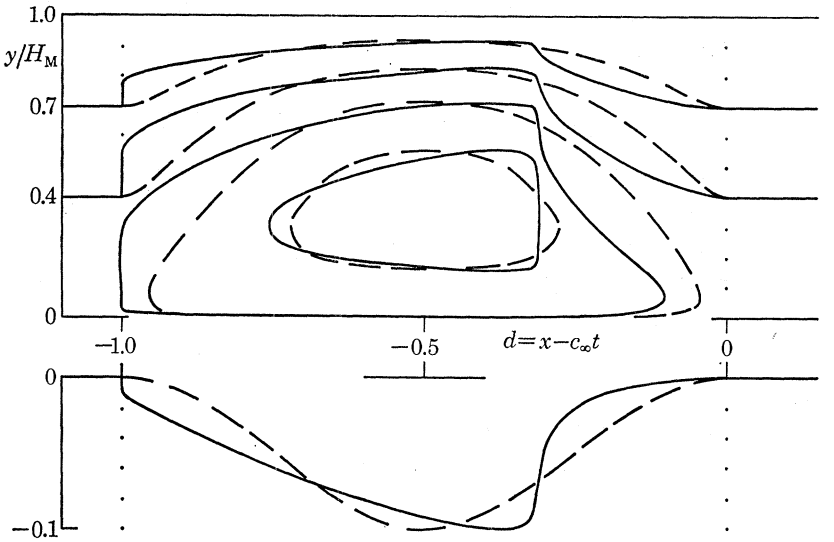

FIGURE 15. The ground pressure signature and typical streamline patterns as viewed by an observer moving with speed c_∞ in the large amplitude wave where the particle trajectories are shown in figure 11. Steepening of the pressure profile occurs both as the pressure is dropping and rising. (For an explanation see the text.) – – –, The situation at $t = 0$; ——, the situation at $t = t_B$.

10. ANALOGOUS BAROTROPIC HYDRAULIC SHEAR FLOWS

10.1. *Introduction*

There are many different hydraulic shear flows for which the governing equations can be transformed either into the set (2.1)–(2.4) or into the set (6.1)–(6.3). The only difference is that the gravity constant g in equation (2.1) is usually replaced by some function of H. Since the results obtained in this paper are also directly applicable to these flows we list some of the more important ones.

10.2. *Axi-symmetric pipe flow*

With a slightly different interpretation of the variables equations (6.1)–(6.3) describe axi-symmetric hydraulic flows down a circular pipe. If u and w denote the axial and radial fluid velocities, the equations governing such flows are

$$\frac{\partial u}{\partial x}+\frac{1}{a}\frac{\partial}{\partial a}(aw) = 0 \tag{10.1}$$

and

$$\frac{\partial u}{\partial t}+u\frac{\partial u}{\partial x}+w\frac{\partial u}{\partial a}+\frac{1}{\rho}\frac{\partial p}{\partial x} = 0, \tag{10.2}$$

where $p = p_0(x, t)$. In addition,

$$w = 0 \quad \text{when} \quad a = 0 \quad \text{and} \quad a = a_1, \tag{10.3}$$

where a_1 is the radius of the pipe. Equations (10.1)–(10.3) are identical with (6.1)–(6.3) with

$$y = \pi(a_1^2-a^2), \quad v = \mathrm{D}y/\mathrm{D}t = -2\pi aw \quad \text{and} \quad H_M = \pi a_1^2. \tag{10.4}$$

The scheme described in § 3 is equivalent to approximating the shear profile in the pipe by a series of parabolic profiles. In particular, the two layer profile discussed in §§ 4–9 is equivalent to the profile shown in figure 16.

When the flow domain is that bounded by two coaxial cylinders of outer radius a_1 and inner radius a_0, y and v are still given by (10.4) but now $H_M = \pi(a_0^2 - a_1^2)$.

10.3. *Incompressible flows between flexible boundaries*

The hydraulic shear flows described in §§ 6 and 10.1 are contained between rigid boundaries. A simple example of a flow adjacent to flexible boundaries that can also be treated by our approach is the incompressible flow between two flexible surfaces that prior to the arrival of the disturbance are parallel planes. During the passage of any disturbance the vertical displacements of these boundaries are known functions of the pressure at the boundaries. If (x, u) are the distance measure and component of fluid velocity in the direction of propagation of the disturbance and if (z, w) are the distance measure and component of fluid velocity normal to the undisturbed boundaries the equations governing such flows are

$$\frac{\partial u}{\partial t} + u\frac{\partial u}{\partial x} + w\frac{\partial u}{\partial z} + \frac{1}{\rho}\frac{\partial p}{\partial x} = 0 \tag{10.5}$$

and

$$\frac{\partial u}{\partial x} + \frac{\partial w}{\partial z} = 0. \tag{10.6}$$

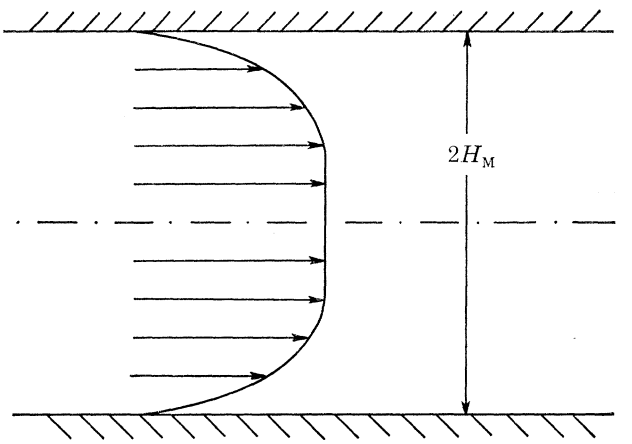

FIGURE 16. Shear profile for the flow in a circular duct for which the analyses in §§ 4–9 are directly applicable.

In addition,

$$p = p_0(x, t). \tag{10.7}$$

These are to be solved subject to the condition that on the lower boundary

$$z = z_0(x, t), \quad w = \frac{\partial z_0}{\partial t} + u\frac{\partial z_0}{\partial x}, \tag{10.8}$$

while on the upper boundary

$$z = z_1(x, t), \quad w = \frac{\partial z_1}{\partial t} + u\frac{\partial z_1}{\partial x}. \tag{10.9}$$

In (10.8) and (10.9), z_0 and z_1 are related to p_0 by the wall equations

$$z_0 = h_0(p_0) \quad \text{and} \quad z_1 = h_1(p_0). \tag{10.10}$$

These can be used to determine a relation between p_0 and

$$H = z_1 - z_0, \tag{10.11}$$

the width of the fluid layer. This relation is written

$$p_0 = \rho G(H). \tag{10.12}$$

The reduction of the system of equations (10.5)–(10.12) to the canonical form (2.1)–(2.4) is achieved by the transformations

$$y = z - z_0(x,t) \quad \text{and} \quad v = \frac{\mathrm{D}y}{\mathrm{D}t} = w - \left(\frac{\partial z_0}{\partial t} + u\frac{\partial z_0}{\partial x}\right). \tag{10.13}$$

Now, though, in (2.1)

$$g = G'(H). \tag{10.14}$$

The result follows by straightforward manipulations.

It should be noted that even when g varies with H, as in (10.14), all of the equations in §§ 2–4 are unchanged. However, some minor changes in some of the constants in §§ 5–9 must be made.

When the flow is axi-symmetric and is contained between two flexible surfaces whose boundaries at any axial distance x are concentric circles whose radii vary in a known way with $p_0(x,t)$ the governing equations are (10.1) and (10.2). These are to be solved subject to the conditions that on the inner wall

$$a = a_0(x,t), \quad w = \frac{\partial a_0}{\partial t} + u\frac{\partial a_0}{\partial x} \tag{10.15}$$

while on the outer wall

$$a = a_1(x,t), \quad w = \frac{\partial a_1}{\partial t} + u\frac{\partial a_1}{\partial x}. \tag{10.16}$$

In addition, the wall equations

$$a_0 = h_0(p_0) \quad \text{and} \quad a_1 = h_1(p_0) \tag{10.17}$$

are known.

In terms of the variables

$$y = \pi(a_1^2 - a^2), \quad v = \frac{\mathrm{D}y}{\mathrm{D}t} = \pi\left[\frac{\partial a_1^2}{\partial t} + u\frac{\partial a_1^2}{\partial x} - 2aw\right] \tag{10.18}$$

and

$$H = \pi[h_1^2(p_0) - h_0^2(p_0)] \tag{10.19}$$

equations (10.1), (10.2), (10.15) and (10.16) are transformed into the set (2.1)–(2.4). Now,

$$g = G'(H) \tag{10.20}$$

where the relation

$$p_0 = \rho G(H) \tag{10.21}$$

is determined from (10.19). Note the special case when $h_0 \equiv 0$. Then the equations describe hydraulic shear flow in a flexible tube.

10.4. *Compressible, isentropic shear flows between flexible boundaries*

Even when the fluid in the problems described in section (10.2) is compressible, the governing equations can still be transformed into the set (2.1)–(2.4) if the flow is isentropic. For example, in the problem governing the flow between almost plane flexible boundaries the only equation that is changed in the set (10.5)–(10.10) is (10.6) which must be replaced by the equation

$$\frac{\partial \rho}{\partial t} + u\frac{\partial \rho}{\partial x} + \rho\left(\frac{\partial u}{\partial x} + \frac{\partial w}{\partial z}\right) = 0. \tag{10.22}$$

In addition, the equation of state for isentropic flow can be written

$$\rho = \rho(p_0). \tag{10.23}$$

The required transformations in this case are

$$y = \rho(z - z_0) \quad \text{and} \quad v = \frac{\mathrm{D}y}{\partial t} = \rho\left[w - \left(\frac{\partial z_0}{\partial t} + u\frac{\partial z_0}{\partial x}\right)\right] + (z - z_0)\left[\frac{\partial \rho}{\partial t} + u\frac{\partial \rho}{\partial x}\right]. \tag{10.24}$$

Also,
$$H = \rho(p_0)\,[h_1(p_0) - h_0(p_0)]. \tag{10.25}$$

In terms of (x, y, u, v) and H the governing equations reduce to the set (2.1)–(2.4) but with

$$g = \frac{1}{\rho}\frac{\mathrm{d}p_0}{\mathrm{d}H}. \tag{10.26}$$

This can be determined as a function of H by using (10.23) and (10.25).

For the special case of compressible shear flow between rigid plates separated by a distance d

$$z_0 = 0 \quad \text{and} \quad z_1 = d. \tag{10.27}$$

Then, according to equations (10.24)–(10.26),

$$y = \rho z, \quad v = \frac{\mathrm{D}y}{\mathrm{D}t} = \rho w + z\left(\frac{\partial \rho}{\partial t} + u\frac{\partial \rho}{\partial x}\right), \tag{10.28}$$

$$H = \rho d \quad \text{and} \quad g = (\rho d)^{-1}\,\mathrm{d}p_0/\mathrm{d}\rho. \tag{10.29}$$

For compressible axi-symmetric flows between flexible walls equations (10.18) and (10.19) must be modified to read

$$y = \pi\rho(a_1^2 - a^2), \quad v = \mathrm{D}y/\mathrm{D}t \tag{10.30}$$

and
$$H = \pi\rho(p_0)[h_1^2(p_0) - h_0^2(p_0)]. \tag{10.31}$$

g is still given by (10.26) but with $p_0(H)$ determined from (10.31).

10.5. *Long gravity waves in a barotropic atmosphere*

Another, rather more complicated, class of flows for which the governing equations reduce to the canonical set (2.1)–(2.4) occur in a barotropic, homentropic (well mixed) atmosphere during the passage of horizontally travelling gravity waves that, to a good approximation, leave the atmosphere in hydrostatic balance during their passage. If x denotes the horizontal distance measure in the direction of travel, and if z is the vertical distance measure the governing equations are

$$\frac{\partial u}{\partial t} + u\frac{\partial u}{\partial x} + w\frac{\partial u}{\partial z} + \frac{1}{\rho}\frac{\partial p}{\partial x} = 0 \tag{10.32}$$

$$\frac{1}{\rho}\frac{\partial p}{\partial z} + \bar{g} = 0 \tag{10.33}$$

and
$$\frac{\partial \rho}{\partial t} + u\frac{\partial \rho}{\partial x} + w\frac{\partial \rho}{\partial z} + \rho\left(\frac{\partial u}{\partial x} + \frac{\partial w}{\partial z}\right) = 0. \tag{10.34}$$

In addition, if
$$i = i(p) \tag{10.35}$$

denotes the enthalpy of the atmospheric gas (the entropy is uniform),

$$\rho^{-1} = \mathrm{d}i/\mathrm{d}p. \tag{10.36}$$

We consider the situation when the flow region is bounded below by a rigid boundary $z = 0$ and above by a free surface, $z = \mathrm{D}(x, t)$, on which the pressure, p_A, is constant. Consequently, equations (10.32)–(10.34) are to be solved subject to the conditions that

$$w = 0 \quad \text{on} \quad z = 0 \tag{10.37}$$

while
$$p = p_\mathrm{A} \quad \text{and} \quad w = \frac{\partial D}{\partial t} + u\frac{\partial D}{\partial x} \quad \text{on} \quad z = D(x, t). \tag{10.38}$$

To transform the above equations to the canonical form (2.1)–(2.4) use (x, t) and

$$y = p_0 - p \tag{10.39}$$

as independent variables where $p_0(x, t)$ denotes the pressure on $z = 0$. As dependent variables use u,

$$v = \mathrm{D}y/\mathrm{D}t \quad \text{and} \quad H(x, t) = p_0 - p_A. \tag{10.40}$$

(y, v) are the well-known sigma variables that are often used by meteorologists (see Phillips 1957). In terms of these variables it can be shown by direct computation that equations (10.32)–(10.34) and the boundary conditions (10.37) and (10.38) transform into the set (2.1)–(2.4) but with

$$g = i'(p_A + H) \tag{10.41}$$

in these latter equations. In terms of the canonical variables,

$$p = p_A + H - y$$

and

$$\bar{g}z = i(p_A + H) - i(p_A + H - y). \tag{10.42}$$

In particular, the depth D of the fluid layer is given in terms of H by

$$\bar{g}D = i(p_A + H) - i(p_A). \tag{10.43}$$

In (10.33), (10.42) and (10.43) $\bar{g}$ denotes the gravity constant.

For isentropic flows of a polytropic gas we can write

$$i = \frac{\gamma}{\gamma - 1}\frac{p_{0\infty}}{\rho_{0\infty}}\left(\frac{p}{p_{0\infty}}\right)^{(\gamma-1)/\gamma}, \quad = \frac{\gamma}{\gamma - 1}RT, \tag{10.44}$$

where $p_{0\infty}$ and $\rho_{0\infty}$ are the pressure and density at the ground ahead of the wave. It then follows from (10.36) and (10.44) that the ground density ρ_0 and the ground temperature T_0 are given in terms of the ground pressure p_0 by the relations

$$\rho = \rho_{0\infty}\left(\frac{p_0}{p_{0\infty}}\right)^{1/\gamma} \quad \text{and} \quad T_0 = T_{0\infty}\left(\frac{p_0}{p_{0\infty}}\right)^{(\gamma-1)/\gamma}. \tag{10.45}$$

H is given in terms of p_0 by (10.40). Off the ground

$$p = p_0\left[1 - \frac{z}{\Delta}\right]^{\gamma/(\gamma-1)}, \quad \rho = \rho_0\left[1 - \frac{z}{\Delta}\right]^{1/(\gamma-1)} \quad \text{and} \quad T = T_0\left[1 - \frac{z}{\Delta}\right], \tag{10.46}$$

where

$$\Delta(x, t) = \frac{\gamma}{\gamma - 1}\frac{p_{0\infty}}{\bar{g}\rho_{0\infty}}\left(\frac{p_0}{p_{0\infty}}\right)^{(\gamma-1)/\gamma}, \quad = \left(\frac{p_0}{p_{0\infty}}\right)^{(\gamma-1)/\gamma}\Delta_\infty. \tag{10.47}$$

Note that equations (10.45)–(10.47) imply that we can write

$$T = T_0(x, t) - T_{0\infty}\, y/\Delta_\infty \tag{10.48}$$

so that, no matter how large the amplitude of the disturbance, in a well-mixed isentropic atmosphere the lapse rate, $T_{0\infty}/\Delta_\infty$, remains constant. This approximation can only be used below the tropopause which is typically around 10 km high. The scale height of the atmosphere, Δ_∞, is typically 28 km.

Some of the work reported in this paper was done while one of the authors (E.V.) was on sabbatical leave at the Department of Applied Mathematics and Theoretical Physics at

Cambridge University. He would like to thank the British Research Council for financial support during this period. He would also like to thank Professor Sir James Lighthill, F.R.S., for his kindness and encouragement.

References

Blythe, P. A., Kazakia, Y. & Varley, E. 1972 *J. Fluid Mech.* **56**, 241.
Blythe, P. A., Kazakia, Y. & Varley, E. 1971 *Tech. Rep. Cent. Applic. Maths, LeHigh Univ.* no. CA-M110-22 (AD)-738548).
Burns, J. C. 1953 *Proc. Camb. Phil. Soc.* **49**, 695.
Davey, A., Hocking, L. M. & Stewartson, K. 1974 *J. Fluid Mech.* **63**, 529.
Hocking, L. M., Stewartson, K. & Stuart, J. T. 1972 *J. Fluid Mech.* **51**, 705.
Phillips, W. A. 1957 *J. Met.* **14**, 184.
Rayleigh, Lord 1880 *Scientific papers*, vol. 1, 474. Cambridge University Press.
Stuart, J. T. 1963 *Laminar boundary layers*. Oxford: Clarendon Press.

Appendix A

To analyse all three families of waves it is convenient to work with the normalized variables

$$A = \frac{\omega}{g}(u_1 - c), \quad B = \frac{\omega}{g}(u_0 - c), \quad C = \frac{\omega}{g}c \quad \text{and} \quad D = \frac{\omega^2}{g}H. \tag{A 1}$$

In terms of these equations (5.3) and (5.4) read

$$\frac{\mathrm{d}A}{\mathrm{d}D} + \frac{\mathrm{d}C}{\mathrm{d}D} + A^{-1} = 0, \quad \frac{\mathrm{d}B}{\mathrm{d}D} + \frac{\mathrm{d}C}{\mathrm{d}D} + B^{-1} = 0 \tag{A 2}$$

and

$$(A-B)^2 = B(A^2 - D). \tag{A 3}$$

When C and D are eliminated (A 2) and (A 3) yield the first order nonlinear equation

$$\frac{\mathrm{d}B}{\mathrm{d}A} = \frac{B^3A + 2AB^2(B-A) + 2B(B-A)^2}{B^3A + (A+B)(A-B)^2}. \tag{A 4}$$

The solutions to this are best described by introducing the parameter τ through the relation

$$A = \tau B. \tag{A 5}$$

When this expression for A is inserted (A 4) yields the equation

$$\frac{\mathrm{d}B}{\mathrm{d}\tau} = -\frac{B}{(\tau-1)}\frac{B\tau(2\tau-3) - 2(\tau-1)^2}{B\tau(2\tau-1) - (\tau-1)^2} \tag{A 6}$$

for $B(\tau)$. (A 3) and (A 5) then imply that

$$D = B^2\tau^2 - (\tau-1)^2 B. \tag{A 7}$$

Also, from (5.2)

$$d = \omega^2 h/g = (\tau-1)\,B. \tag{A 8}$$

Equations (A 5)–(A 8) determine A, B, D and d as functions of the parameter τ. To obtain an equation for C use (A 6), (A 7) and the second of equations (A 2) to obtain the equation

$$\frac{\mathrm{d}C}{\mathrm{d}\tau} = -\frac{B}{(\tau-1)}\frac{3B\tau + (\tau+2)(\tau-1)^2}{B\tau(2\tau-1) - (\tau-1)^2}. \tag{A 9}$$

The integral curves of (A 6) are shown schematically in figure A 1. There are two singular points

$$S_1\colon (B,\tau) = (0,1) \quad \text{and} \quad S_2\colon (B,\tau) = (\tfrac{9}{4}, -\tfrac{1}{2}). \tag{A 10}$$

Since S_2 lies in the region where $D < 0$ it is of no interest here since we assume that $\omega > 0$. S_1, though, is the central point of the diagram. All acceptable integral curves corresponding to forward and backward waves pass through this point where

$$A = B = D = d = 0. \tag{A 11}$$

One of these curves is the hyperbola $\tau(1-B) = 1,$ (A 12)

which is the exact solution discussed by Blythe *et al.* (1972). Along this curve $d \equiv D$ so that the whole flow region is one of constant shear. Another integral curve is

$$\tau \equiv 1. \tag{A 13}$$

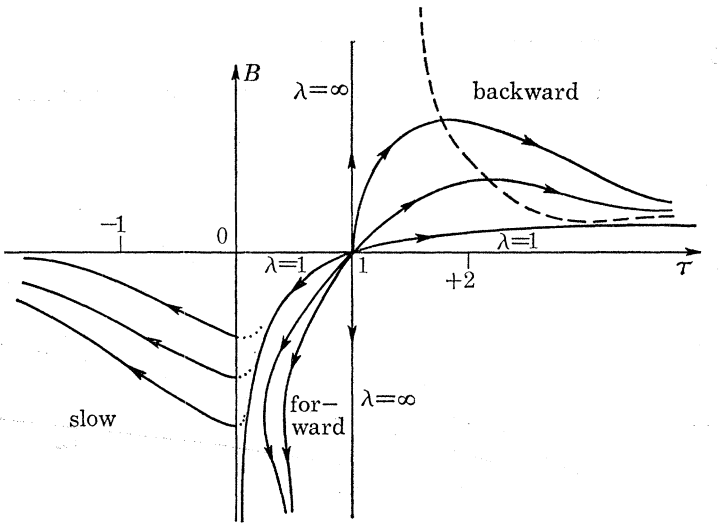

FIGURE A 1. The integral curves of equation A 6 for the backward, forward and slow waves. At the broken curve $\mathrm{d}B/\mathrm{d}\tau = 0$.

Along this curve $d \equiv 0$ so that the fluid is not sheared. All other acceptable curves lie between the curves (A 12) and (A 13). These curves are conveniently parameterized by

$$\lambda = \mathrm{d}B/\mathrm{d}\tau \quad \text{at} \quad S_1. \tag{A 14}$$

In the vicinity of this point

$$B = \lambda(\tau - 1) + (3 - 4\lambda)(\tau - 1)^2 + \ldots. \tag{A 15}$$

The integral curve (A 12) corresponds to $\lambda = 1$, the integral curve (A 13) corresponds to $\lambda = \infty$. For the backward wave $\tau \geqslant 1$, for the forward wave $\tau \leqslant 1$. At the broken curve in figure A 1

$$\mathrm{d}B/\mathrm{d}\tau = 0.$$

Figures A 2–A 4 show typical variations of B and C with D in the forward and backward waves. At the broken curve $\mathrm{d}B/\mathrm{d}H = 0$.

The integral curves for the slow waves occupy the quadrant where $(\tau, B) < 0$ in figure A 1. Each curve intersects the axis $\tau = 0$ at a distinct value of B, $= -\Lambda$ say, and as $\tau \to -\infty$ asymptotes to the axis $B = 0$. The parameter Λ can take any value in the range $[0, \infty]$. Note that according to (A 5), (A 7) and (A 8)

$$\text{at} \quad \tau = 0, \quad d = D = -B = \Lambda. \tag{A 16}$$

A study of (A 6) and (A 8) shows that $-B$ and d decrease monotonically from Λ at $\tau = 0$ to zero at $\tau = -\infty$. Thus, Λ is the maximum value these variables can take in the wave. (A 6) and (A 7)

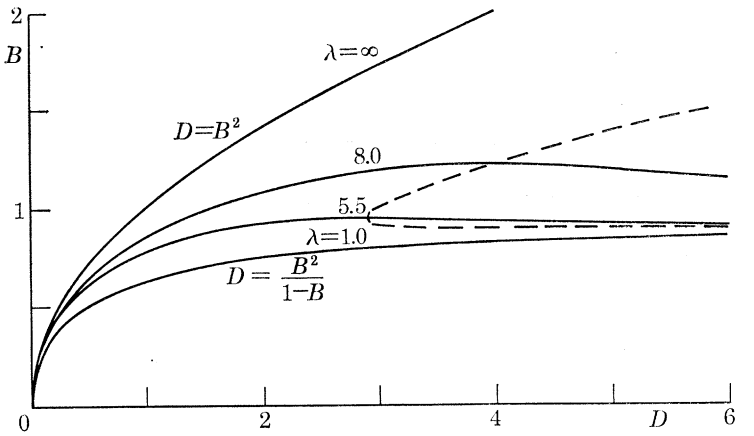

FIGURE A 2. Variations in B with D in the backward wave. Along the broken curve $dB/dD = 0$.

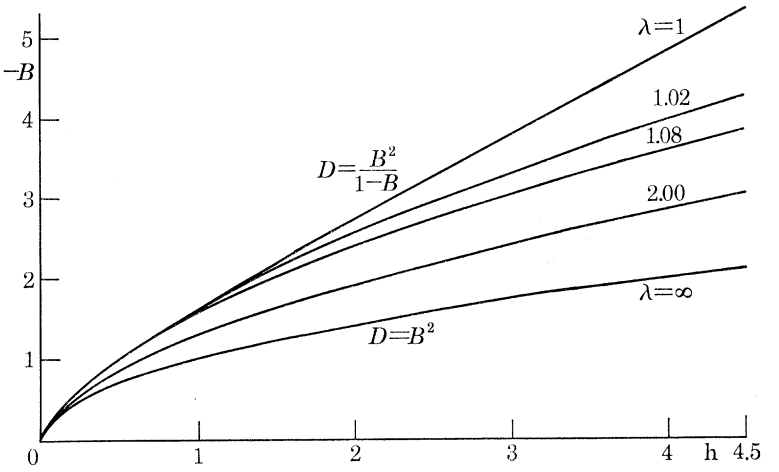

FIGURE A 3. Variations in B with D in the forward wave.

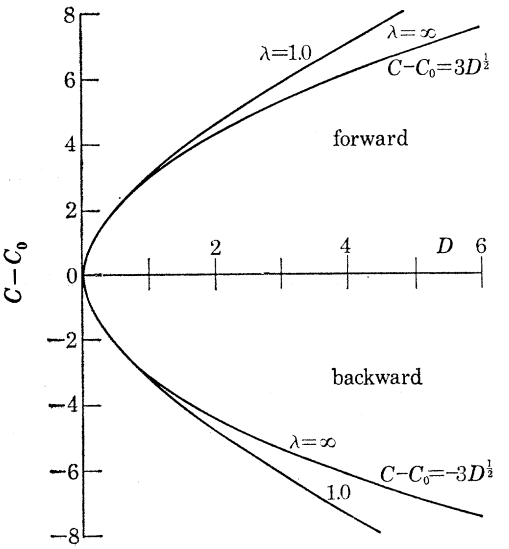

FIGURE A 4. Variations of C with D in forward and backward waves.

imply that D increases monotonically from Λ at $\tau = 0$ to some *finite* value at $\tau = -\infty$. Thus, Λ is the minimum value of D that can occur in the wave. Note that d, the height of the interface separating the sheared and unsheared fluid, can vary over the full range $0 \leqslant d \leqslant D$ as D varies over a finite range. This is also true for the critical level y_c which, according to (4.1) and (A 1) is given by

$$\omega^2 y_c/g = -B. \tag{A 17}$$

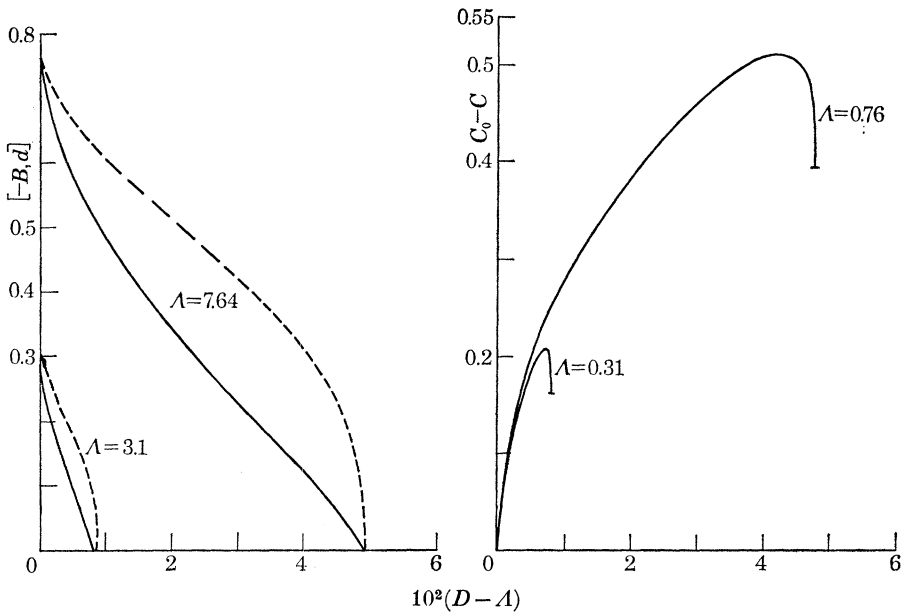

FIGURE A 5. Typical variations of $(\omega^2/g)\,[y_c, h] = [-B, d]$ with D in the slow waves. ——, The height of the critical level; – – –, the height of the interface separating sheared and unsheared flow.

FIGURE A 6. Typical variations of C with D in slow waves.

Figures A 5 and A 6 show typical variations of $\omega^2 y_c/g = -B(D)$, $\omega^2 h/g = d(D)$ and $C(D)$ as D varies over its maximum range. C_0 is the value of C at $\tau = 0$. Note that C is not a monotonic function of D as it is for the forward and backward waves. Also, the amplitude dispersion frequency $\mathrm{d}C/\mathrm{d}D$ is unbounded when D attains its maximum value. When this occurs the critical height and the dividing interface are at ground level.

The internal waves discussed in section 4 are obtained in the limit as $\Lambda \to 0$. Then,

$$\text{since} \quad |B| \leqslant \Lambda \quad \text{for all} \quad -\infty \leqslant \tau \leqslant 0 \tag{A 18}$$

equation (A 6) implies that the dominant uniformly valid approximation to $B(\tau)$ satisfies the equation

$$\frac{\mathrm{d}B}{\mathrm{d}\tau} + 2\frac{B}{\tau - 1} = 0. \tag{A 19}$$

Also, from (A 9), the dominant uniformly valid approximation to $C(\tau)$ satisfies the equation

$$\frac{\mathrm{d}C}{\mathrm{d}\tau} - \frac{(\tau+2)}{(\tau-1)}B = 0. \tag{A 20}$$

These integrate to give

$$B = -\Lambda(\tau-1)^{-2} \quad \text{and} \quad C - C_0 = [(\tau-1)^{-1} + \tfrac{3}{2}(\tau-1)^{-2} - \tfrac{1}{2}]\,\Lambda. \tag{A 21}$$

Since (A 7) and (A 8) imply that

$$r = h/H = d/D \to -(\tau - 1)^{-1} \quad \text{as} \quad \Lambda \to 0, \tag{A 22}$$

the dominant approximations to B and C can be written

$$B = -\Lambda r^2 \quad \text{and} \quad C - C_0 = [\tfrac{3}{2}r^2 - r - \tfrac{1}{2}]\,\Lambda. \tag{A 23}$$

Also, it follows from (A 5), (A 22) and (A 23) that

$$A = [r - r^2]\,\Lambda. \tag{A 24}$$

Finally, if the expression (A 7) for D is written

$$D = -(\tau - 1)^2 B\left[1 - B\left(\frac{\tau}{\tau - 1}\right)^2\right] \tag{A 25}$$

it follows from (A 21) and (A 6) that

$$D = \Lambda[1 + O(\Lambda)] \tag{A 26}$$

and then from (A 22) that

$$d = \Lambda r[1 + O(\Lambda)] \quad \text{as} \quad \Lambda \to 0. \tag{A 27}$$

Thus, as r varies over the full range $[0, 1]$ as τ varies over the range $[-\infty, 0]$ d varies over the full range $[0, \Lambda]$ although D does not change perceptibly from Λ. When the expressions (A 24), (A 25), (A 26) and (A 27) are written in dimensional variables they imply the relations (5.4)–(5.5). To obtain the $O(\Lambda^2)$ correction to H given by (5.6) equation (A 6) must be used to obtain B to $O(\Lambda^2)$ and (A 7) and (A 8) to obtain B and d to $O(\Lambda^2)$.

PHILOSOPHICAL TRANSACTIONS OF THE ROYAL SOCIETY A MATHEMATICAL, PHYSICAL & ENGINEERING SCIENCES